GDOT Research Project 14-18

FINAL REPORT

Implementation of Optimal Parameter Settings in GDOT's Current Ramp Metering Operation

OFFICE OF PERFORMANCE-BASED MANAGEMENT AND RESEARCH

15 KENNEDY DRIVE

FOREST PARK, GA 30297-2534

<table>
<tr><td colspan="2">1. Report No.
FHWA-GA-19-1418</td><td>2. Government Accession No.</td><td>3. Recipient's Catalog No.</td></tr>
<tr><td colspan="3">4. Title and Subtitle
Implementation of Optimal Parameter Settings in GDOT's Current Ramp Metering Operation</td><td>5. Report Date
February, 2019
6. Performing Organization Code</td></tr>
<tr><td colspan="3">7. Author(s)
Jorge A. Laval, Ph.D., Angshuman Guin, Ph.D., Bhargava Chilukuri, Ph.D., and Hyun W. Cho</td><td>8. Performing Organization Report No.
14-18</td></tr>
<tr><td colspan="3">9. Performing Organization Name and Address
School of Civil and Environmental Engineering
Georgia Institute of Technology
790 Atlantic Dr.
Atlanta, GA 30332-0355</td><td>10. Work Unit No. (TRAIS)
11. Contract or Grant No.
PI# 0012795</td></tr>
<tr><td colspan="3">12. Sponsoring Agency Name and Address
Office of Performance-based Management and Research
15 Kennedy Drive
Forest Park, GA 30297-2534</td><td>13. Type of Report and Period Covered
November 2014 – February 2019
14. Sponsoring Agency Code</td></tr>
<tr><td colspan="4">15. Supplementary Notes
Prepared for the Georgia Department of Transportation</td></tr>
<tr><td colspan="4">16. Abstract
The objective of this study is to optimize the parameter settings for the local ramp metering control system currently in operation in the Metro Atlanta freeway network. The study corridor is Eastbound/Southbound I-285 between GA 400 and I-20. Using a stochastic simulation-based optimization framework that combines microsimulation model GTsim and a genetic algorithm-based optimization module, we determine the optimal parameter values of the ramp-metering control system. We generate optimal ramp metering values for 11 ramp-metering locations. The results of this project are expected to improve ramp metering efficiency and mitigate freeway congestion.</td></tr>
<tr><td colspan="2">17. Key Words
Ramp Metering, ALINEA, Genetic Algorithm Optimization</td><td colspan="2">18. Distribution Statement</td></tr>
<tr><td>19. Security Classif. (of report)
Unclassified</td><td>20. Security Classif. (of this page)
Unclassified</td><td>21. No. of pages
74</td><td>22. Price</td></tr>
</table>

Form DOT F 1700.7 (8-72) Reproduction of completed page authorized

Table of Contents

List of Figures

List of Tables

EXECUTIVE SUMMARY

The objective of this project is to optimize the parameter settings for the ramp metering control systems in operation on the EB/SB I-285 study corridor between GA-400 and US-78. This study was accomplished with the simulation-based optimization framework GTsim, modified to account for the existing control system configuration. The project developed parameter settings for the MaxView software that GDOT acquired for the freeway and arterial signal management.

We found that each local ramp metering system has different critical density values, so it needs to be optimized carefully. This study analyzed extensive traffic data to generate origin-destination (O-D) flows of the study corridor. We used tube counters (flow) data for on- and off- ramps and NaviGAtor (flow and speed) data for the mainline freeway to estimate travel time of each O-D.

This study also developed a Genetic Algorithm-based optimization method to generate optimal parameters of the RM system. We found that optimal RM reduces almost 5 % of total travel time compared to the current control method. These savings are not trivial considering that the upstream sections of the corridor (near Peachtree Industrial Blvd and North Peachtree Rd) gets completely congested by the end of the rush hour period. Since many ramps of the study corridor operate at minimum rate after a certain time, it is safe to say that most of the benefits of parameter optimization are realized during the congestion build-up phase.

From the optimal parameter and the critical density, we generated recommended metering rates for each location, which GDOT can readily implement in MaxView.

1 Introduction

The main challenge of effective ramp metering is to develop optimal strategies that not only enhance the impact of the individual ramp meters in its vicinity but maximize system benefits. Researchers have developed several ramp metering algorithms for real-time management of ramp meters (Masher et al., 1975; M Papageorgiou, Hadj-Salem, & Blosseville, 1991; E Smaragdis, Papageorgiou, & Kosmatopoulos, 2004; Emmanouil Smaragdis & Papageorgiou, 2003), but there is little guidance on critical issues such as hours of operation, determining thresholds, and efficient methodology for on-ramp queue-flush management. This problem is very challenging and location specific that even the Ramp Management and Control Handbook (Leslie Jacobson, Stribiak, Nelson, & Sallman, 2006) only makes qualitative statements in this regard.

The research team completed Georgia Department of Transportation (GDOT) Research Project "Development of Optimal Ramp Metering Strategies" (Guin & Laval, 2013) in the context of the System-Wide Adaptive Ramp-Metering (SWARM), which was acquired by GDOT and has yet to be implemented. The project produced GTsim, a ramp-metering and a simulation-based optimization platform that combines the microscopic traffic flow model, which accurately predicts traffic dynamics under ramp-metering (Laval & Leclercq, 2008) with the Genetic Algorithm optimization framework. This combination allowed us to successfully identify optimal parameters for the ramp metering system within the study corridor.

The optimization of existing control system is very important. To identify the optimal settings of the existing ramp metering algorithms being applied in the field today by the Traffic Management Center (TMC), this research project implemented and optimized the findings and tools developed in the "Development of Optimal Ramp Metering Strategies" study (Guin & Laval, 2013).

The objective of this study is to optimize the parameter settings for the local ramp metering control system currently in operation in the Metro Atlanta freeway network. This is accomplished with the simulation-based optimization framework GTsim, developed in the GDOT Research Project 07-22, modified to account for the existing control system configuration. The study corridor is the 19.25-mile, EB/SB I-285 corridor between GA 400 and I-20.

2 Literature Review

Ramp meters break up the vehicle platoons entering the freeway to enable smooth merging of the on-ramp flows with the freeway flows and prevent capacity drop. They also control excessive inflows into the freeway to avoid freeway queues from blocking the off-ramps. This is important because higher outflows mean lower delay. Towards this end, this section presents a brief overview of the isolated and coordinated ramp metering methods.

2.1. Isolated Metering

Isolated metering strategies are classified in 4 categories, based on the underlying method; linear programming (Iida Y., Hasegawa T., Asakura Y., 1989; Wattleworth, 1965; Yuan L.S. and Kreer, 1968), control theory (Masher et al., 1975; M Papageorgiou et al., 1991; E Smaragdis et al., 2004; Emmanouil Smaragdis & Papageorgiou, 2003), neural networks (Zhang & Ritchie, 1997), and fuzzy-logic (Bogenberger, Vukanovic, & Keller, 2002; Taylor, Meldrum, & Jacobson, 1998). However, methods based on linear programming and control theory are popular and field implemented extensively.

Fixed-time isolated control began with the seminal work of Wattleworth (Wattleworth, 1965) who derived optimal metering rates using steady-state vehicle conservation across ramps and linear programming, using historical data. Later, Yuan and Kreer (Yuan L.S. and Kreer, 1968) and others build on the Wattleworth's methodology to maximize the flow and balance the ramp queues. Papageorgiou (Markos Papageorgiou, 1980) improved Wattleworth's method by relaxing the steady-state condition. Masher et.

al. (Masher et al., 1975) developed the first traffic responsive control for isolated metering; demand-capacity and percentage occupancy methods as presented below:

Consider a typical freeway-ramp section and the traffic parameters as shown in Figure 1, where *q(.)* and *r(.)* represents the average flow and *o(.)* represents average occupancy. The demand-capacity strategy states that the metering rate at time *k* is:

$$\boldsymbol{r}(k) = \begin{cases} Q - q_{in}(k-1), & O_{out} < O_{cr} \\ q_{min}, & otherwise \end{cases}$$

Where Q and O_{cr} are the desired flow and occupancy (which are typically set to capacity and critical occupancy) and q_{min} is the minimum metering rate.

The philosophy of the percentage-occupancy strategy is similar to the demand-capacity strategy and only defers in its implementation. Instead of measuring upstream flow, $q_{in}(.)$, the percentage-occupancy strategy uses upstream occupancy to estimate the flow. Moreover, the downstream occupancy is also measured at the upstream detector. Therefore, the percentage-occupancy strategy only needs one freeway detector (upstream of the ramp location) to determine metering rate.

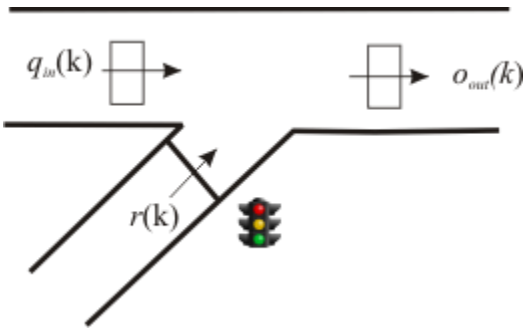

Figure 1 Freeway-ramp configuration and parameters

Papapageorgiou et. al. (M. Papageorgiou, Hadj-Salem, & Middelham, 1997; M Papageorgiou et al., 1991) developed the popular feedback controller, ALINEA, that aims to maintain critical occupancy at the merge location. According to ALINEA:

$$\boldsymbol{r}(k) = \boldsymbol{r}(k-1) + \boldsymbol{K}_R(\boldsymbol{O}_{cr} - \boldsymbol{O}_{out}(k))$$

where K_R is the regulating parameter, which is in the range of 60-70 vehicle/hr. ALINEA feedback law is simple, flexible, robust, and provides smooth transitions during congestion build up and dissipation. ALINEA was field implemented extensively and found to perform better than the fixed-time plans (M. Papageorgiou et al., 1997; Markos Papageorgiou, Kosmatopoulos, Papamichail, & Wang, 2008). To overcome implementation issues, several variations of ALINEA such as AD-ALINEA (Adaptive Strategy to Dynamically Calculate Critical Occupancy), AU-ALINEA (upstream-measurement-based version of the AD-ALINEA), FL-ALINEA (flow-based ALINEA), UP-ALINEA (upstream-occupancy-based), UF-ALINEA (upstream-flow-based), and X-ALINEA/Q (combination of any of the preceding strategies with queue control) were developed (Emmanouil Smaragdis & Papageorgiou, 2003; Wang, Kosmatopoulos, Papageorgiou, & Papamichail, 2014).

2.2. Coordinated Metering

Coordinated metering methods can be broadly divided into three categories: Multivariable control, optimal control, and rule-based control.

Multivariable Control

Papageorgiou (Diakaki & Papageorgiou, 1994; Markos Papageorgiou, Blosseville, & Haj-Salem, 1990; Markos Papageorgiou, Jean-marc, & Hadj-salem, 1989) derived a linear quadratic integral control for a system of ramp meters using linear quadratic optimization theory. METALINE, as it was called, is a vectorized extension of ALIEA as shown below:

$$\boldsymbol{r}(k) = \boldsymbol{r}(k-1) + \boldsymbol{K}_1(\mathbf{o}(\mathrm{k}) - \mathbf{o}(k-1)) + \boldsymbol{K}_2(\widehat{\boldsymbol{O}} - \mathbf{O}(k))$$

Where $\boldsymbol{r}(k)$ indicates a set of controlled on-ramps $\boldsymbol{r} = [r_1, r_2, \dots r_n]^T$, $\boldsymbol{o}(k)$ indicates a set of state measurements $\boldsymbol{o} = [o_1, o_2, \dots o_m]^T$, and $\boldsymbol{O}(k)$ indicates a subset of state measurements $\boldsymbol{o}$ for which target occupancies are available $\widehat{\boldsymbol{O}} = [\hat{O}_1, \hat{O}_2, \dots \hat{O}_n]^T$. Finally, $\boldsymbol{K_1}$ and $\boldsymbol{K_2}$ are the calibrated gain matrices. While field applications in Paris (Markos Papageorgiou et al., 1990, 1989) and Amsterdam (Diakaki & Papageorgiou, 1994) proved that METALINE is simple and robust, its performance was found to be sensitive to the gain matrices used.

Rule-Based Metering

Rule-based algorithms are popular, and field implemented extensively. Some of the popular rule-based algorithms include Zone algorithm (Stephanedes, 1994), ALINEA

(M Papageorgiou et al., 1991), Minnesota Zone algorithm (Liu, Wu, & Michalopoulos, 2007), Linked-ramp metering algorithm (Banks, 1993), Denver Helper ramp algorithm (Lipp, Corcoran, & Hickman, 1991), Seattle Bottleneck algorithm (L Jacobson, Henry, & Mehyar, 1989), and SWARM (Paesani, Kerr, Perovich, & Khosravi, 1997).

The Zone algorithm (Stephanedes, 1994) divides the freeway into zones with their upstream boundary in free-flow and downstream boundary a bottleneck. The algorithm uses conservation to maintain each zone at desired level. Later improvements to the algorithm balance the freeway efficiency and ramp delay to maximize freeway flow.

In the Heuristic Ramp-Metering Coordination (HERO) algorithm, each ramp is outfitted with an ALINEA algorithm. When the queue on a ramp exceeds a threshold, it becomes a "master" control and controls some upstream ramps to reduce the queues at the Master ramp. The aim of this algorithm is to efficiently use all the space available on the network but does not optimize for the freeway-ramp system.

Similar to the Zone algorithm, System Wide Area Ramp-Metering (SWARM) algorithm divides the corridor into segments. The control operates on global and local level, with the former doing the forecasting and apportioning and the latter providing local responsive metering. The most restrictive of the two metering rates is used.

One of the drawbacks of these methods is that they all generally employ ad hoc feedforward control to achieve a target flow. As they are reactive, they resort to queue flush when the queue constraints are violated.

This page is intentionally left blank.

3. Optimization Framework

The simulation-based optimization framework for determining optimal parameter values is shown in Figure 2.

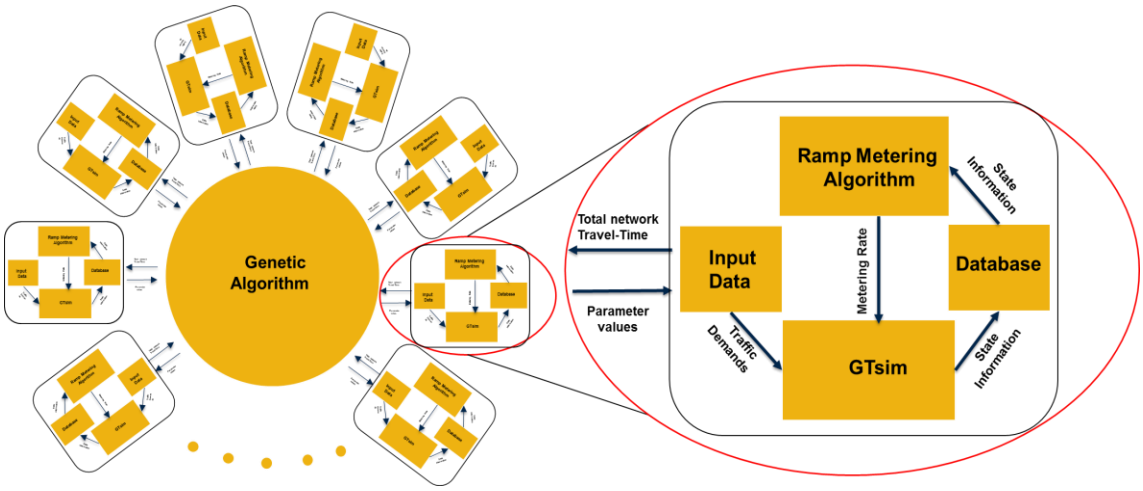

Figure 2 Optimization Framework

Two main components of this framework are the Generic-Algorithm-based (GA-based) optimizer and GTsim module. The optimizer will provide a set of parameter values that are utilized by the GTsim module to estimate the total travel time that will be sent back to the optimizer. The GTsim application will provide continuous state information to the ramp metering algorithm that calculates metering rates based on the state information and the parameters provided by the GA based optimizer. The sections below describe GTsim and GA based optimizer as implemented in this study.

3.1. GTsim Application

GTsim, which is built based on a kinematic wave model, is the first one of its kind proven to replicate traffic dynamics during congestion. *GTsim* implements the latest lane-changing models, which significantly improved understanding of traffic congestion. Specific explanations on GTsim modules were introduced in the final report of the "Development of Optimal Ramp Metering Strategies" study (Guin & Laval, 2013).

In GTsim, we generated the 19.25-mile corridor as in the project's objective; see Figure 3.

3.2. Genetic Algotirhm

The objective of this project is to find optimal combination of parameters of ramp metering for the study corridor. As the solution space is large, simulation-based optimization, genetic algorithm play an important role in converging to the global optimum. Parameters of the genetic algorithm were described in the final report of the "Development of Optimal Ramp Metering Strategies" study (Guin & Laval, 2013).

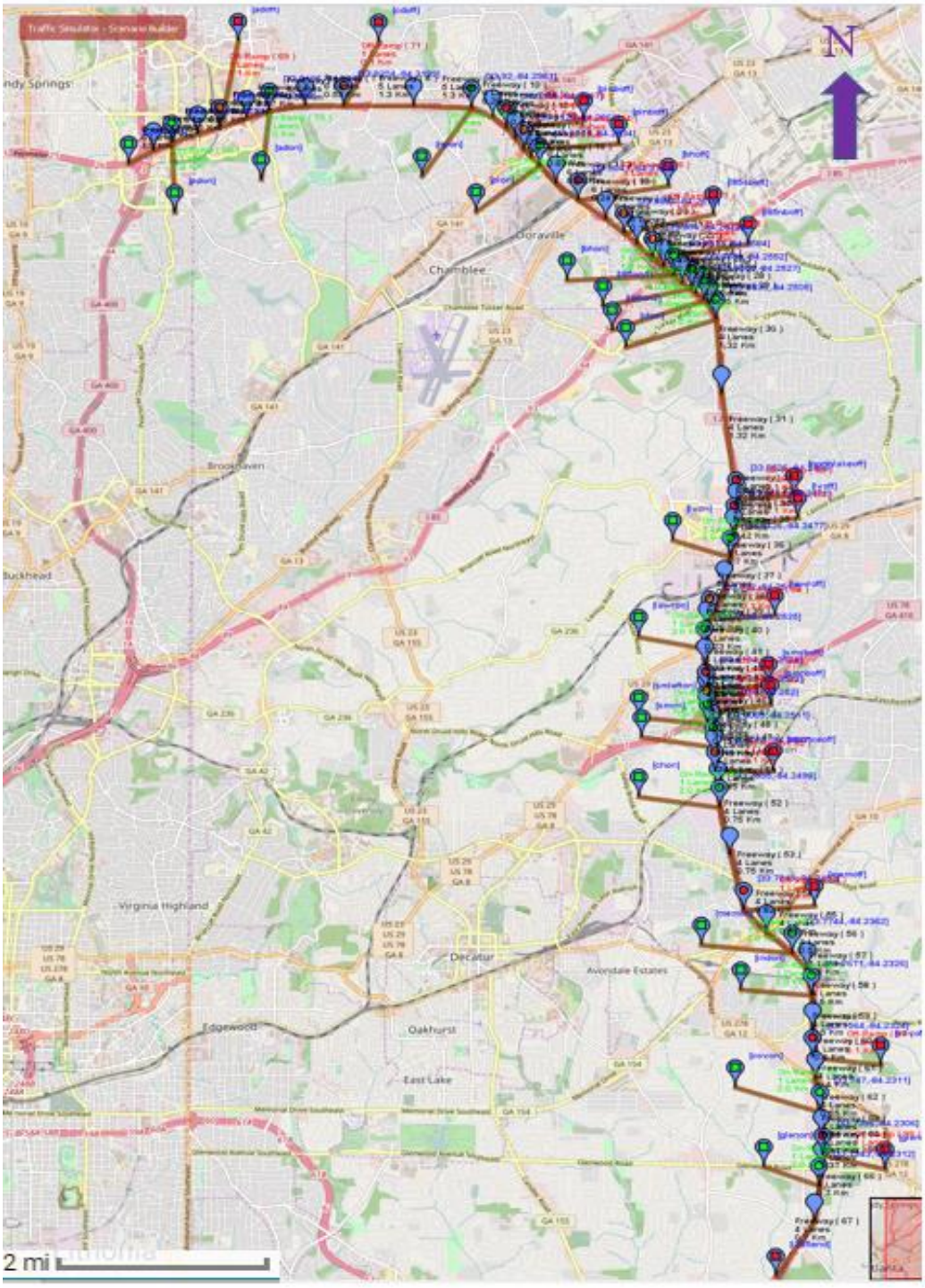

Figure 3 The network of the study corridor (I-285 Eastbound/Southbound) shown in GTsim application.

This page is intentionally left blank.

4. Methodology

4.1. Study corridor

The study involved the selection of a 19.25-mile-long I-285 East Bound/South Bound corridor between GA-400 and I-20. This corridor contains thirteen ramp meter systems and 20 variable speed limits (see Figure 4). From typical traffic congestion characteristics from Google Maps and historical data of VDS (see Appendix), this study focuses on the onset period of evening peak congestion.

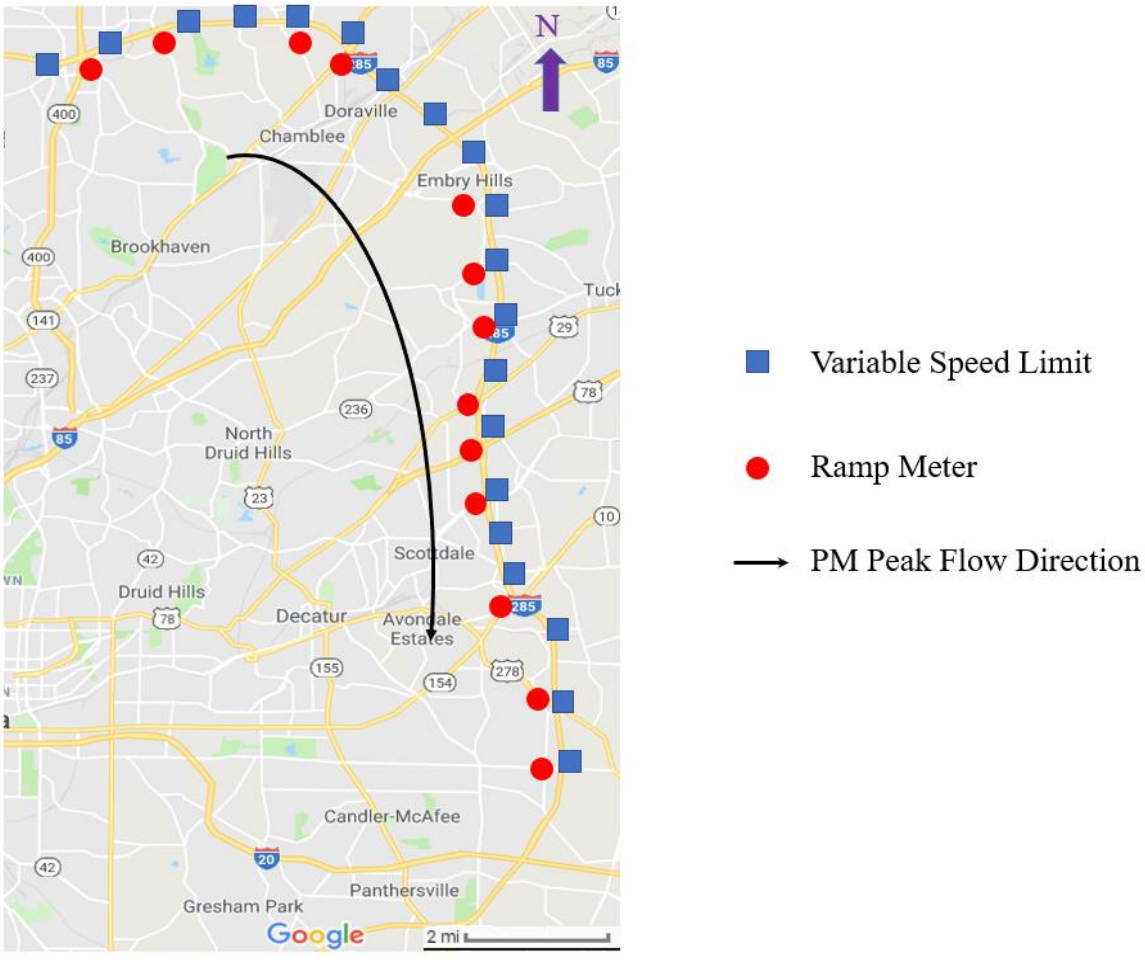

Figure 4 Study Corridor

The study corridor has the following seventeen entry locations (referred to as "origins" for the OD terminology) that feed traffic to the network:

- Upstream Freeway, Peachtree Dunwoody Road, Ashford Dunwoody Road, North Peachtree Road, Peachtree Industrial Parkway, Buford Highway, the I-85 Connector, Chamblee Tucker Road, Lavista Road, Lawrenceville Highway, WB Stone Mountain Freeway (left lane merge), EB Stone Mountain Freeway, Church Street, Memorial Drive, Indian Creek Station Connector, Covington Highway, Glenwood Road.

The corridor has the following seventeen exit locations (referred to as "destinations"):

- Ashford Dunwoody Road, Chamblee Dunwoody Road, SB Peachtree Industrial Parkway, NB Peachtree Industrial Parkway, Buford Highway, the SB I-85 Connector, the NB I-85 Connector, Northlake Parkway, Lavista Road, Lawrenceville Highway, WB Stone Mountain Freeway, EB Stone Mountain Freeway, East Ponce de Leon Avenue, Memorial Drive, Covington Highway, Glenwood Road, Downstream Freeway.

4.2. Traffic Data Analysis

4.2.1. Data

Within the 19.25-mile study corridor, this study used 52 GDOT NaviGAtor's Vehicle Detection System (VDS) (Figure 5, Figure 6) data that collected 20-second interval volume, speed, and occupancy (hereafter referred to as the "VDS data"). This study extracted the 52-stations VDS data during a one-month period (April 2016).

Five-minute volume data for 48 hours were measured using traffic tube counts (see Figure 7, GDOT traffic tube counts for specific locations). Tube counters could be installed in all on- and off- ramps in the corridor except for six locations: the NB GA-400 on-ramp, the SB Peachtree Industrial Blvd off-ramp, the Buford Hwy on-ramp, the I-85 connector on-ramp, the WB Stone Mountain Fwy connector on-ramp, I-20 off-ramp. Notice that most of these locations are freeway interchanges with no metering, and that this missing data was estimated as explained next).

As traffic volume data are the main input variables of this simulation case study and containing the volume data for all ramps is critical, this study focused on identifying the five-minute traffic volume of the missing locations for the same 48 hours by analyzing VDS data and the upstream and downstream ramps of the missing locations. For example, for the SB Peachtree Industrial Blvd off-ramp, we compared the VDS data of detector ID 2850034, 2850036, 2850037, which are the NB Peachtree Industrial Blvd off-ramp, and the Peachtree Industrial Blvd on-ramp, respectively. We assumed that the mainline volume on the corridor would be conserved by adding or subtracting the ramp

volume. However, a comparison of tube count data and the VDS data resulted in unreasonable ramp volumes (negative values) for the missing ramps.

The unrealistic ramp volumes could have resulted from the low-quality VDS data. For example, some detectors lost the data of one lane out of five or six lanes. We also tried to compensate for these missing lanes by multiplying the ratio of the missing lanes. However, we needed the lane distributions for each location to obtain the volume of correct whole lanes, which is beyond the scope of this study.

Because of these limitations, this study excluded the most upstream and downstream missing ramps, the GA-400 on-ramp, and the I-20 off-ramp. This exclusion, however, did not affect the system corridor because the GA-400 on-ramp does not contain a ramp-metering system, and the I-20 off-ramp does not affect congestion in the corridor.

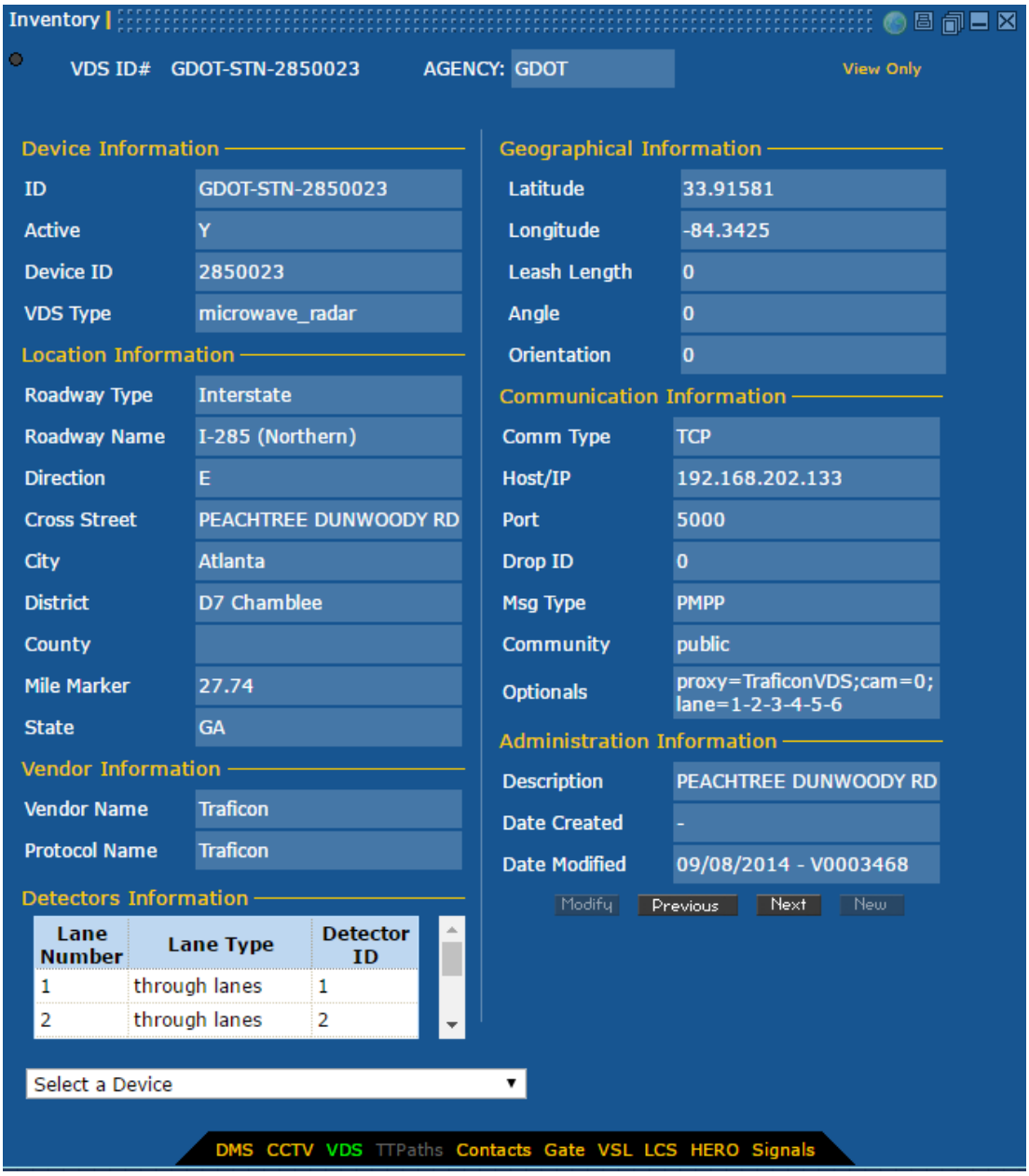

Figure 5 GDOT NaviGAtor video detection system (VDS)

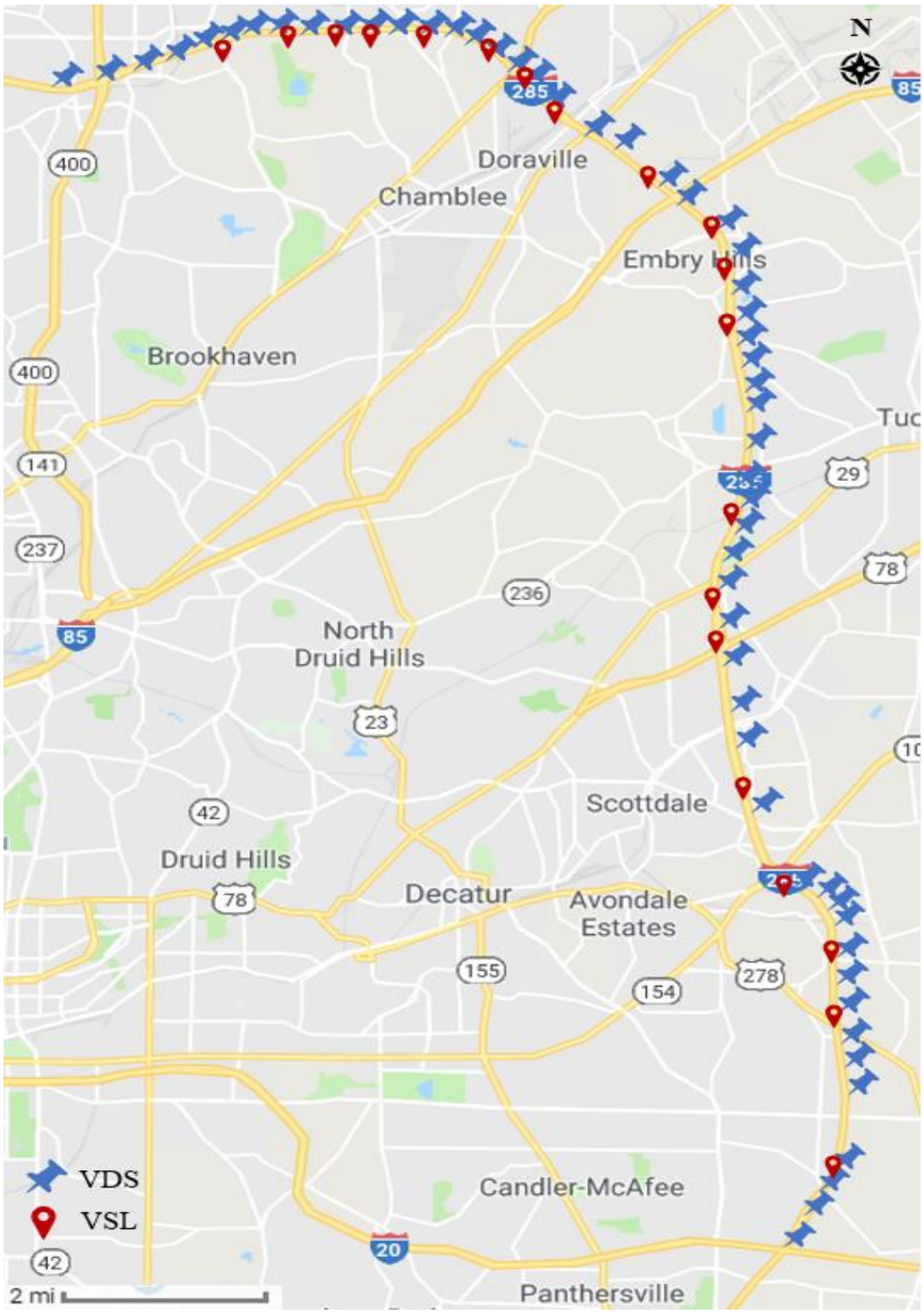

Figure 6 Locations of GODT NaviGAtor's Vehicle Detection System (blue) and Varaible speed limit (red) on Google Map.

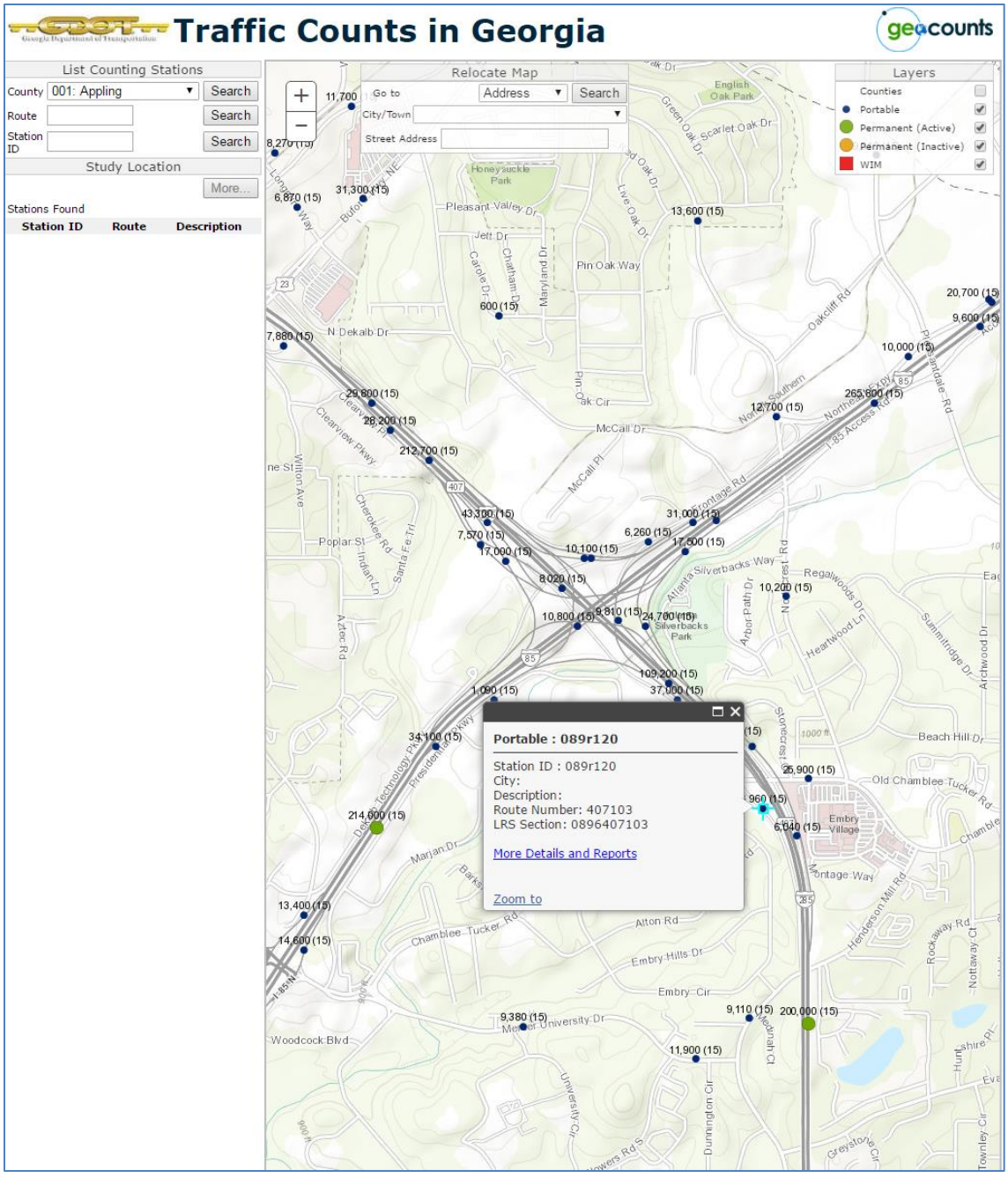

Figure 7 GDOT traffic tube counts

4.2.2. Data Processing for Origin Destination Matrix Estimation

Rationally estimated origin-destination traffic volume matrix is essential in this simulation-based research. Figure 8 describes the steps of the O/D matrix estimation. We first extracted the traffic volume of the on-ramp (origin) and the off-ramp (destination) for the time periods of interest (PM peak) from the tube counts and the VDS volume data. We also calculated the travel time across each origin and destination using the space-mean speed that was converted from VDS speed data.

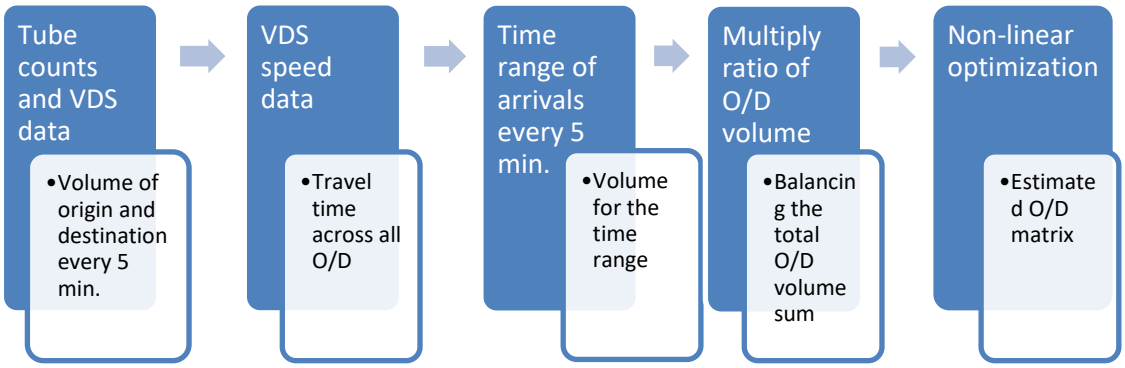

Figure 8 Flow chart of O/D matrix estimation

Using these travel time data, we produced the possible time range of the arrival of the origin traffic. For example, for the I-285 downstream freeway destination, the earliest time of arrival would be the time that the first vehicle departed from the closest origin, Glenwood Road, and arrived at the destination from the beginning of the time period. Similarly, the latest time of arrival would be the time that the last vehicle departed from the farthest origin, I-285 Upstream freeway, and arrived at the destination from the end of the time periods. Using these possible time ranges of arrival, we calculated the arrival traffic volume for each destination.

The target time periods of our research are before the onset of the off-peak. From the typical traffic data of Google Maps, we found that off-peak congestion on our research corridor formed before 3:00 PM. Therefore, we chose 2:30 PM to 3:30 PM (60 minutes) as the time periods for this study.

The time periods of the origin traffic were set at 60 minutes. However, the calculated possible time periods of destination traffic were longer than 60 minutes as they were affected by congestion. To meet the total sum of the origin and destination traffic, we adjusted the destination traffic volume by multiplying the ratio of the sum of the origin volume to the sum of the possible destination volume.

After matching the sum of the origin and destination traffic volume, we estimated the O/D matrix using a nonlinear optimization method. We explain the assumptions and constraints of this optimization method using the simple network below (Figure 9).

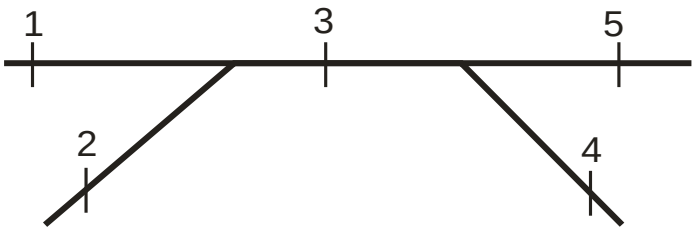

Figure 9 Sample network for OD estimation

This network consists of two origins (1, 2) and two destinations (4,5). From observed data (i.e., tube counts, VDS), the volumes of each origin and destination are generated (1-A, 2-B, 4-C, and 5-D). The volume of section 3 is calculated by adding the volumes of sections 1(A) and 2(B). To calculate the destination specific volumes, we generated the O/D matrix as Table 1. Constraints are that the sum of each row and

column volumes are close to the total estimated volume. For example, a volume that is generated from section 1(a) is composed of volumes heading to 4 ($\boldsymbol{\alpha}$) and 5($\boldsymbol{\beta}$). In this case, we set constraint $\boldsymbol{\alpha + \beta \leq a}$. Other rows and columns work in a similar manner. Subsequently, we generated a volume-calculation table, Table 2, and then we can calculate the O/D matrix using the optimization function. In the mathematical formulation, the objective function and constraints are described as follows.

$$obj.: \ min.(A-a)^2 + (B-b)^2 + (A+B-a-b)^2 + (C-c)^2 + (D-d)^2$$

Subject to $\alpha + \beta \leq a, \gamma + \delta \leq b, \ \alpha + \gamma \leq c, \ \beta + \delta \leq d$

Table 1 Sample O/D calculation table

O \ D	**4**	**5**	**TARGET**	**SUM**
1	α	β	A	a
2	γ	δ	B	b
TARGET	C	D		
SUM	c	d		

Table 2 Sample calculated and observed flow

	Calculated	Observed	Square of Differences
1	a	A	$(\boldsymbol{A}-\boldsymbol{a})^{\boldsymbol{2}}$
2	b	B	$(\boldsymbol{B}-\boldsymbol{b})^{\boldsymbol{2}}$
3	a+b	A+B	$(\boldsymbol{A}+\boldsymbol{B}-\boldsymbol{a}-\boldsymbol{b})^{\boldsymbol{2}}$
4	c	C	$(\boldsymbol{C}-\boldsymbol{c})^{\boldsymbol{2}}$
5	d	D	$(\boldsymbol{D}-\boldsymbol{d})^{\boldsymbol{2}}$

We used the computer program Generalized Reduced Gradient Algorithm (Lasdon, Fox, & Ratner, 1974), which is useful for solving the nonlinear optimization problem. The objective function of our problem is to minimize the total sum of the squared differences of the estimated volume (last column of Table 3), and the constraints are the sums of each cell of rows and columns (see Figure 10 O/D matrix). In Table 3, the green cells represent origin traffic, and the pink cells indicate destination traffic. In Figure 10, the gray cells must be zero because these destinations are upstream of the origins. With the algorithm, we found that the objective value decreased to a two-digit value.

Table 3 Flow calculation

Link	Ramps	Calculated Flow	Observed Flow	Difference	Diff. sqrd.
1	U/S Fwy	7914	7914	0	0
2	Peachtree Dunwoody	1030	1030	0	0
3		8944	8944	0	0
4	Ashford Dunwoody	1317	1317	0	0
5		7627	7627	0	0
6	Ashford Dunwoody	1279	1279	0	0
7		8906	8906	0	0
8	Chamblee Dunwoody	1099	1099	0	0
9		7807	7807	0	0
10	North Peachtree	978	978	0	0
11		8785	8785	0	0
12	SB P'tree Ind.	189	189	0	0
13		8596	8596	0	0
14	NB P'tree Ind.	1492	1492	0	0
15		7104	7104	0	0
16	P'tree Ind.	1963	1963	0	0
17		9067	9067	0	0
18	Buford Hwy	577	577	0	0
19		8490	8490	0	0
20	SB I-85	1440	1440	0	0
21		7050	7050	0	0
22	NB I-85	3181	3181	0	0
23		3869	3869	0	0
24	Buford Hwy	411	411	0	0
25		4280	4280	0	0
26	I-85	3941	3941	0	0
27		8221	8221	0	0
28	Chamblee Tucker	428	428	0	0
29		8649	8649	0	0
30	Northlake Pkwy	1055	1055	0	0
31		7594	7594	0	0
32	Lavista	996	996	0	0
33		6598	6598	0	0
34	Lavista	1063	1063	0	0
35		7661	7661	0	0
36	Lawrenceville Hwy	647	647	0	0
37		7014	7014	0	0
38	Lawrenceville Hwy	502	502	0	0
39		7516	7516	0	0
40	Stone Mt.	910	910	0	0
41		6606	6606	0	0
42	Stone Mt. EB	1276	1276	0	0
43		5330	5330	0	0
44	Stone Mt. Left merge	1017	1017	0	0
45		6347	6347	0	0
46	Stone Mt.	587	587	0	0
47		6934	6934	0	0
48	E Ponce De Leon	664	664	0	0
49		6270	6270	0	0
50	Church St.	382	382	0	0
51		6652	6652	0	0
52	Memorial Dr.	1008	1008	0	0
53		5644	5644	0	0
54	Memorial Dr.	891	891	0	0
55		6535	6535	0	0
56	Indian Creek	21	22	1	1
57		6556	6557	1	0
58	Covington	666	666	0	0
59		5891	5891	0	0
60	Covington	593	593	0	0
61		6484	6484	0	0
62	Glenwood	484	484	0	0
63		5999	6000	1	1
64	Glenwood	507	508	1	1
65		6506	6508	2	4
66	I-20	3203	3200	-3	9
67	D/S Fwy	3303	3300	-3	9

Origin/Destination		Ashford Dunwoody	Chamblee Dunwoody	SB P'tree Industrial	NB P'tree Industrial	Buford Hwy	SB I-85	NB I-85	Northlake pkwy	Lavista	LAWRENCE VILLE HWY	STONE MOUNTAIN FWY	STONE MOUNTAIN FWY EB	EAST PONCE DE LEON AVE	Memorial	Covington	Glenwood	I20	d/s Fwy	Target	Sum
		4	6	8	10	12	14	16	22	24	26	28	30	34	36	40	42	44	46		
u/s Fwy	1	1316	984	189	1258	1	1104	1196	114	99	533	130	120	232	121	0	0	298	219	7914	7914
P'tree Dunwoody	3	1	68	0	136	7	101	523	0	2	8	2	1	6	0	1	0	88	86	1030	1030
Ashford Dunwoody	5		47	0	67	36	98	786	0	1	4	0	26	3	0	1	0	109	99	1279	1279
N. P'tree Rd	7			0	30	22	72	654	0	1	4	0	25	3	0	2	1	85	79	978	978
P'tree Industrial	11					512	65	22	174	152	47	201	246	0	212	21	310	2	0	1963	1963
Buford Hwy	17								24	15	0	21	44	2	13	0	1	159	132	411	411
I-85 C/D SYS	19								722	714	12	464	615	295	386	11	0	270	453	3941	3941
CHAMBLEE TUCKER RD	21								22	12	2	9	43	1	14	0	0	160	165	428	428
Lavista Rd	25										36	57	103	36	73	8	2	365	381	1063	1063
Lawrenceville Hwy	27											24	52	0	23	0	0	222	180	502	502
Stone Mt. FWY Left	31													68	92	0	0	361	496	1017	1017
Stone Mt. FWY	33													18	41	10	67	199	252	587	587
Church St.	35														32	11	78	117	145	382	382
Memorial Dr.	37															601	1	140	149	891	891
Indian Creek	39															0	0	21	0	22	21
Covington	41																25	290	278	593	593
Glenwood	43																	319	188	508	507
	Target	1317	1099	189	1492	577	1440	3181	1055	996	647	910	1276	664	1008	666	484	3200	3300	8	
	Sum	1317	1099	189	1492	577	1440	3181	1055	996	647	910	1276	664	1008	666	484	3203	3303		0
		1317	1099	189	1492	577	1340	3081	955	896	547	810	1176	564	908	566	384	2929	3183		

Figure 10 O/D matrix

4.2.3. Calibration and Validation

GTsim has several parameters that must be calibrated (Chilukuri, Laval, & Guin, 2014). The parameters are categorized into capacity parameters (i.e., free-flow speed, jam density, and wave speed), lane-changing parameters (i.e., longitudinal distance between a vehicle and an exit ramp, tau (i.e., time to execute a lane-changing maneuver), epsilon (i.e., relaxation speed gap), and driver behavior parameters (friction speed). These calibrated parameters are summarized in Table 4. We used all parameter values in Table 4 for the entire corridor, except the value for the parameter of the longitudinal distance between a vehicle and an exit ramp. For some sections of the study corridor, the higher value of this parameter was needed to replicate feasible congestion propagation.

Table 4 Calibrated Parameters

Calibrated Parameter	Parameter Value
Free-flow speed	100 *km/hr*
Jam density	150 *veh/km*
Wave speed	20 *km/hr*
Longitudinal distance between a vehicle and an exit ramp	2 (4) *km*
Tau (time to execute a lane-changing maneuver)	4 *s*
Epsilon (relaxation speed gap)	2
Friction speed	20 *km/hr*

We validated the model by comparing the speed contour maps of (a) NaviGAtor's VDS data (2016/04/12) and (b) GTsim (see Figure 11), which used the estimated O/D flow of the same day data. In Figure 11, the color legend shows the speed scale (unit: *km/hr*). Note that in the speed plot of NaviGAtor (Figure 11 (a)), vehicle speeds over 100 (*km/hr*) are capped at 100 (*km/hr*) to meet the free-flow speed of GTsim. We found that in the real-world corridor on the date (Figure 11 (a)), congestion formed around the 34-mile post area at about 2:45 PM and around the 38-mile post area at about 3:30 PM. We confirmed similar patterns in the GTsim plots (Figure 11 (b)).

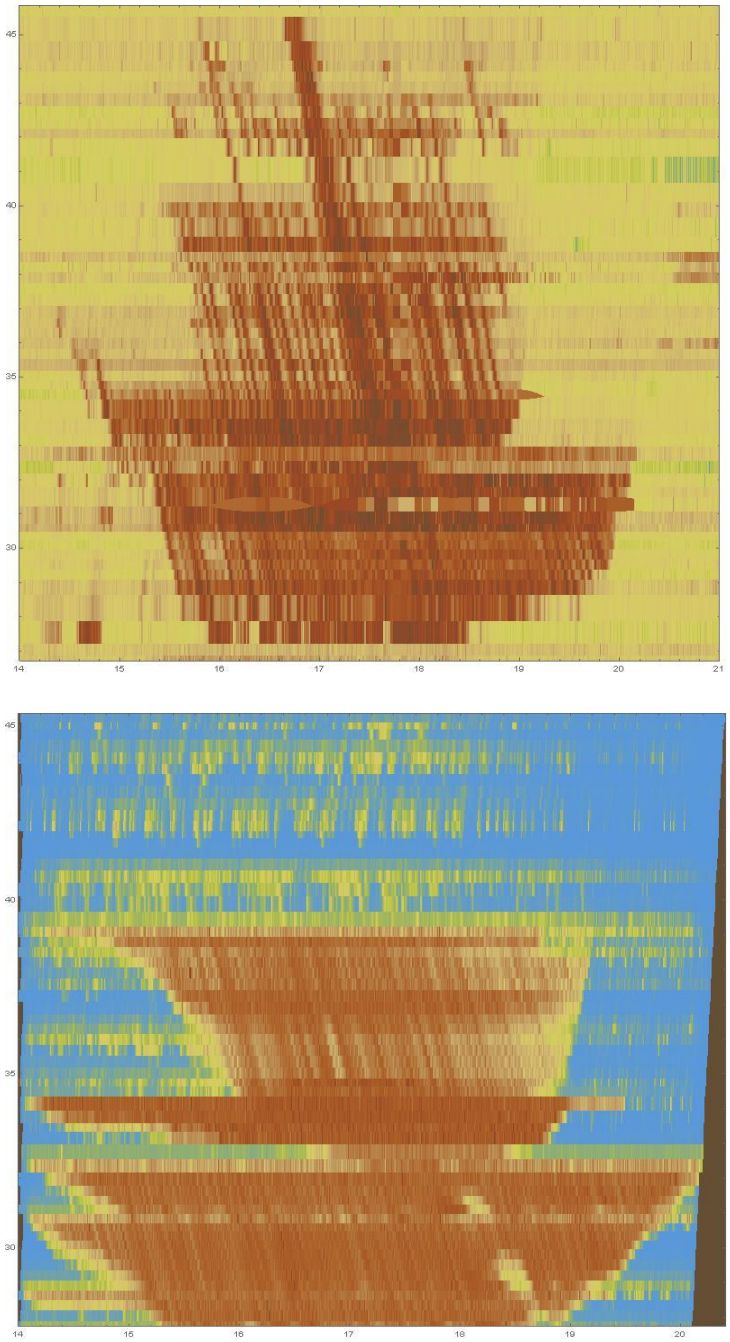

Figure 11 (a) Time Space Speed map of NaviGAtor (upper row, field data) (b) Time Space Speed map of GTsim (lower row, simulation). In the map, x-axis is the time, y-axis is the location. Blue represents high speed while brown represents low speed.

4.2.4. Critical Parameters

In this project, we aim to produce optimal metering rates for each on-ramp meter system. GDOT implemented ALINEA algorithm, which are noted as below

$$\boldsymbol{r}(t) = \boldsymbol{r}(t-1) + K_R\big(\widehat{\boldsymbol{o}} - \boldsymbol{o}_{out}(t)\big).$$

In this equation, $\widehat{\boldsymbol{o}}$ is a critical occupancy (density) that is characterized by location. To obtain this value for each location, we plotted flow-density (q-k) curves using NaviGAtor data (in Appendix). As NaviGAtor data produce flow, speed, and occupancy for 20-second, we combined those data to 5-minute data. We also converted time-mean speed to space-mean speed. After that, we produced density by dividing flow to space-mean speed.

4.3. Traffic Data Analysis

The strategy development and evaluation is an iterative process. The number of allowable values of each of the eleven K_R parameters evaluated in this study which corresponds to a total of 85,899,300,000,000,000,000 combinations of parameter values. Determining the optimal set of parameter values from this huge set is extremely time consuming even with any sophisticated search algorithm. Using the genetic algorithm, we selected optimal solution (combination of the eleven K_R parameters). With the same method, the research team also investigated optimal queue flush parameters, which are maximum and minimum critical density of designated location.

This page is intentionally left blank.

5. Results and Discussion

5.1. Simulation Optimization Result

The results of the simulation-optimization for three cases (no control, the RM control only, the VSL-RM control) are summarized in Table 5. We found that the VSL-RM with optimized parameters outperforms the RM-control-only model with its optimized parameters in terms of reducing total travel time.

Table 5 Travel time (vehicle hours) comparison of no control, the RM control

Case	System	Ramp	Freeway
No control	6561	175	6386
RM control	6254	194	6061
	(4.7%)	(-10.9%)	(5.1%)

Figure 12 show the speed contour maps of each control case. In the figure, we found that most congestion arises upstream of the 32-milepost. The VSL in this study corridor is located at the 34-milepost, and the target bottleneck location is downstream of the 35-milepost, highlighted by the red oval line in the figures. Both controls reduce congestion in the target area. The main benefits of the controls are that they delay the bottleneck formation time and lessen the severity of the bottleneck (passing speed).

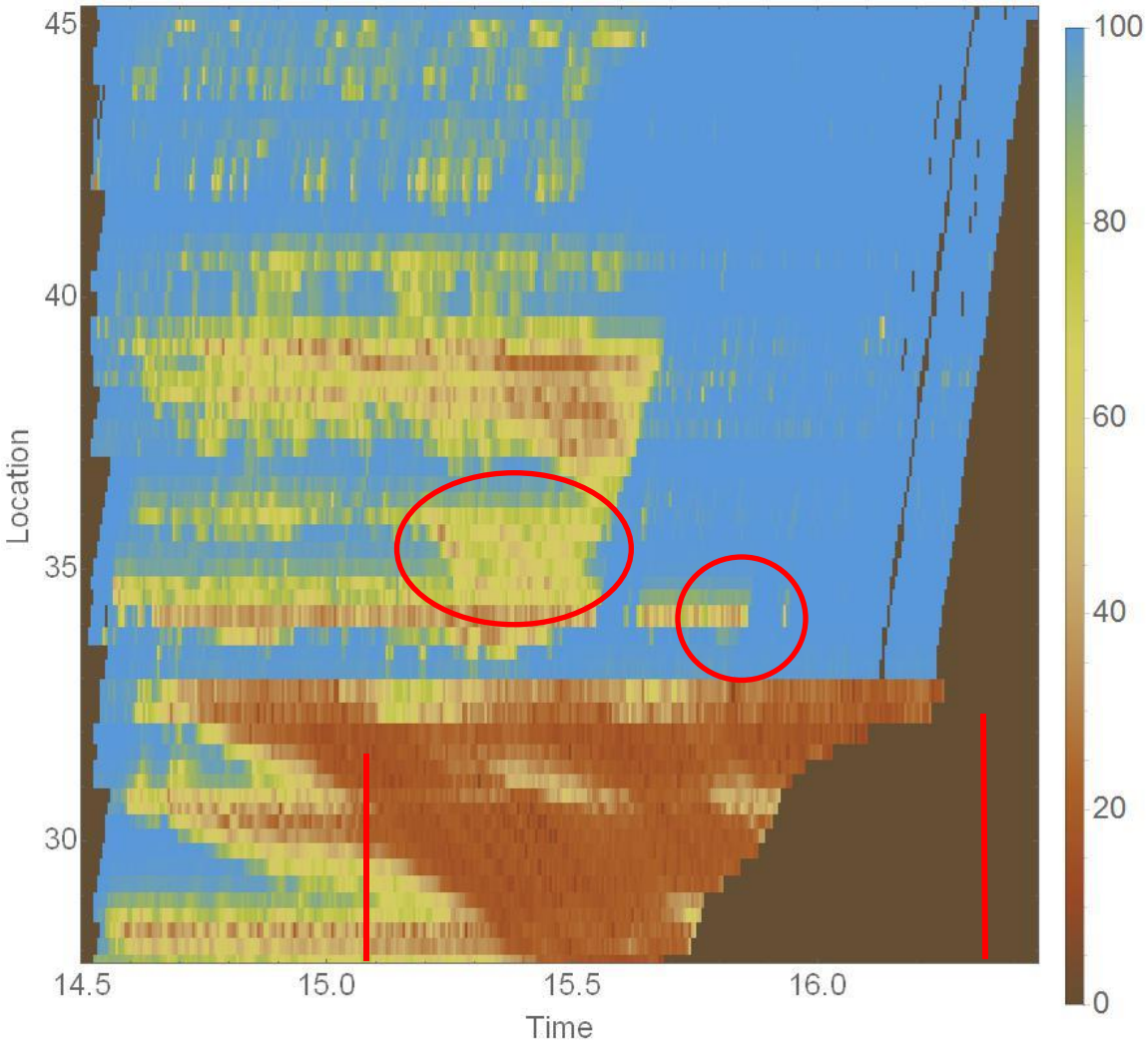

Figure 12 Speed contour map of the no control case. Red circles mean low speed areas to be compared with other figures.

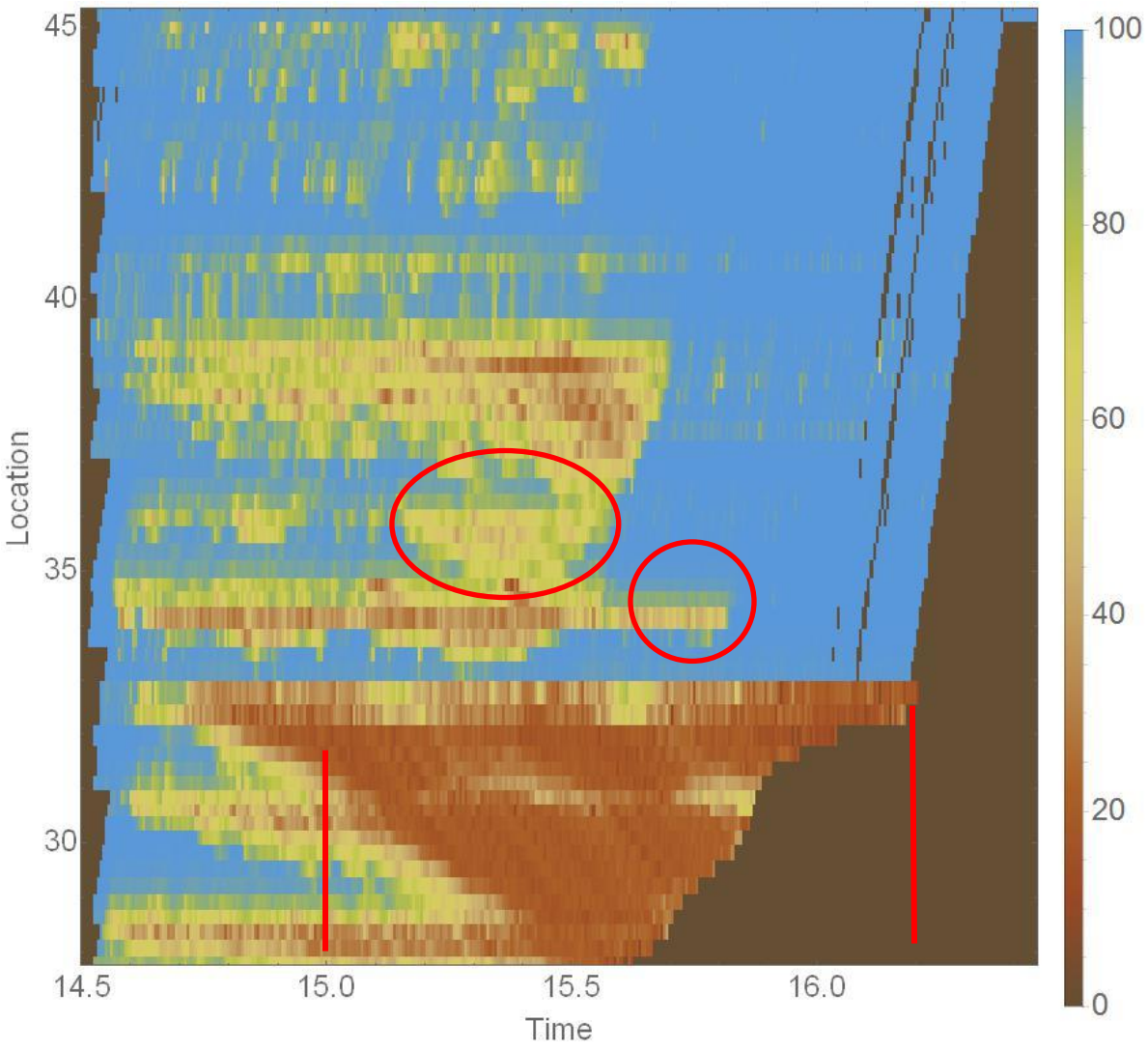

Figure 13 Speed contour map of the RM only control case. Red circles mean low speed areas to be compared with other figures. The congestion is reduced compared to Figure 12.

5.2. Optimal Parameter Values

Based on all possible values for K_R parameters and queue flush density parameters, the solution space was still very large. Therefore, the optimal values of parameters were determined using a different set of GA parameters. A population of 30 and a mutation rate of 0.4 were used and the GA was run for 300 generations. The 15th percentile values of all the generations are plotted in Figure 14 that shows the convergence of GA over generations.

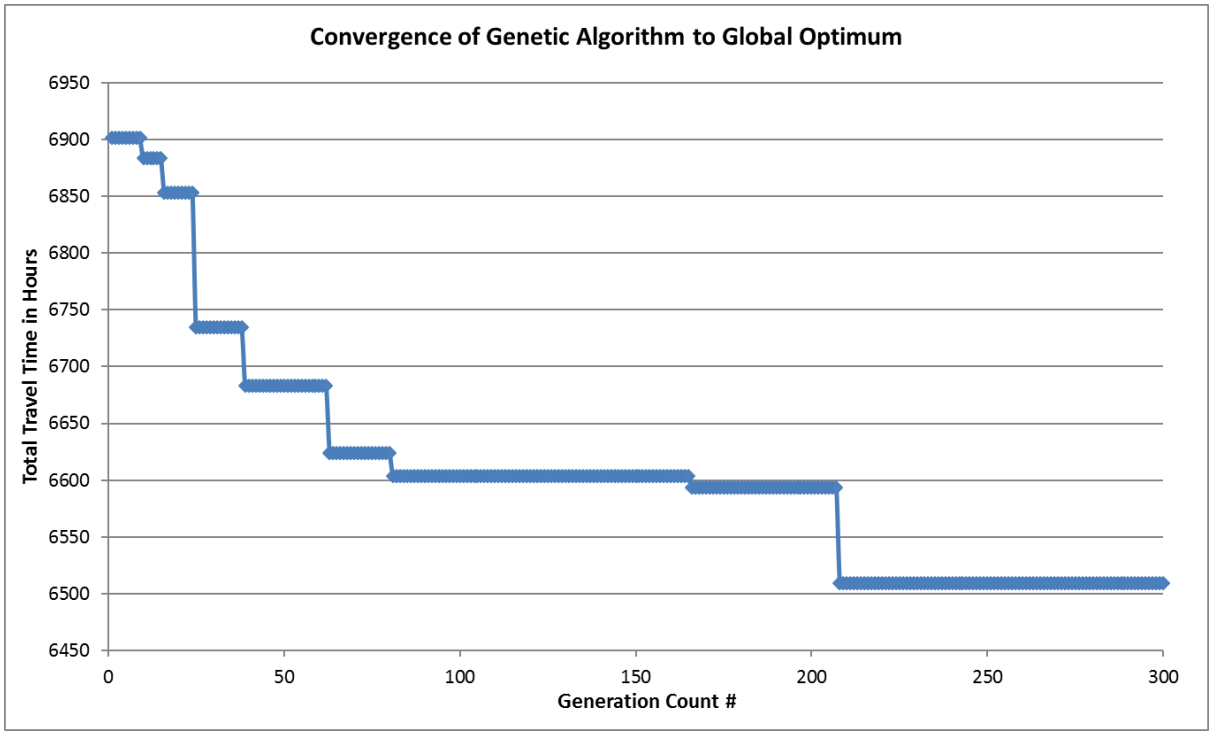

Figure 14: GA Convergence to global optimal over successive generations

Figure 14 shows that after 208 generations, the algorithm converged to a minimum. To confirm that it is the global minima, tens of thousands combination of allowable

values of impact parameters were simulated. It is found that the minimum obtained from the GA after 200 generations was indeed the global minimum. Thus, it was confirmed that the GA parameters used above would converge to the global minimum.

After obtaining optimal K_R parameters, we performed same GA test for queue flush density parameters. Table 4 describes these optimal parameter values.

Table 6 Optimal Parameter Values

Location	K_R	Critical Density (veh/km/lane)	Queue Flush Max. Density (veh/km/lane)	Queue Flush Min. Density (veh/km/lane)
Peachtree Dunwoody Rd	139	20	76	28
Ashford Dunwoody Rd	137	20	75	30
North Peachtree Rd	144	20	74	18
Peachtree Industrial Blvd	87	18	82	15
Chamblee Tucker Rd	59	20	91	9
Lavista Rd	152	18	76	30
Lawrenceville Hwy	147	20	87	5
Church St	86	25	63	12
Memorial Dr	97	25	89	7
Covington Hwy	155	25	84	23
Glenwood Rd	94	23	66	20

5.3. MaxView implementation of Optimal Metering Rates

In this section we provide the necessary input information for GDOT to implement the optimal settings found in our study within the current version of MaxView. Notice that the current version of MaxView does not have the capabilities of implementing real-time control such as ALINEA, and therefore the results in the previous section cannot be directly implemented in the current system. However, in the new version of MaxView that is about to be implemented by GDOT this will be possible. In the meantime, the following tables are approximations of our results that can be implemented in the current system.

5.3.1. Peachtree Dunwoody Rd

K_R=139, Critical Density = 20 (*veh/km/lane*), Maximum rate =1800 *veh/hr*, Minimum rate = 400 *veh/hr*

Table 7 Peachtree Dunwoody Rd Ramp Metering

Rate (veh/hr)	Density (veh/km/ln)
1800	5 or less
1800	6
1800	7
1800	8
1800	9
1800	10
1800	11
1600	12
1450	13
1300	14
1150	15
1000	16
850	17
700	18
550	19
400	20 or more

5.3.2. Ashford Dunwoody Rd

K_R=137, Critical Density = 20 (*veh/km/lane*), Maximum rate =1800 *veh/hr*, Minimum rate = 400 *veh/hr*

Table 8 Ashford Dunwoody Rd Ramp Metering

Rate (veh/hr)	Density (veh/km/ln)
1800	5 or less
1800	6
1800	7
1800	8
1800	9
1800	10
1800	11
1600	12
1450	13
1300	14
1150	15
1000	16
850	17
700	18
550	19
400	20 or more

5.3.3. North Peachtree Rd

K_R=144, Critical Density = 20 (*veh/km/lane*), Maximum rate =1800 *veh/hr*, Minimum rate = 400 *veh/hr*

Table 9 North Peachtree Rd Ramp Metering

Rate (veh/hr)	Density (veh/km/ln)
1800	5 or less
1800	6
1800	7
1800	8
1800	9
1800	10
1800	11
1600	12
1450	13
1300	14
1150	15
1000	16
850	17
700	18
550	19
400	20 or more

5.3.4. Peachtree Industrial Blvd

K_R=87, Critical Density = 18 (*veh/km/lane*), Maximum rate =1700 *veh/hr*, Minimum rate = 400 *veh/hr*

Table 10 Peachtree Industrial Blvd Ramp Metering

Rate (veh/hr)	Density (veh/km/ln)
1700	5 or less
1600	6
1500	7
1400	8
1300	9
1200	10
1100	11
1000	12
900	13
800	14
700	15
600	16
500	17
400	18 or more

5.3.5. Chamblee Tucker Rd

K_R=59, Critical Density = 20 (*veh/km/lane*), Maximum rate =1700 *veh/hr*, Minimum rate = 800 *veh/hr*

Table 11 Chamblee Tucker Rd Ramp Metering

Rate (veh/hr)	Density (veh/km/ln)
1700	5 or less
1640	6
1580	7
1520	8
1460	9
1400	10
1340	11
1280	12
1220	13
1160	14
1100	15
1040	16
980	17
920	18
860	19
800	20 or more

5.3.6. Lavista Rd

K_R=152, Critical Density = 18 (*veh/km/lane*), Maximum rate =1800 *veh/hr*, Minimum rate = 400 *veh/hr*

Table 12 Lavista Rd Ramp Metering

Rate (veh/hr)	Density (veh/km/ln)
1800	5 or less
1800	6
1800	7
1800	8
1800	9
1600	10
1450	11
1300	12
1150	13
1000	14
850	15
700	16
550	17
400	18 or more

5.3.7. Lawrenceville Hwy

K_R=147, Critical Density = 20 (*veh/km/lane*), Maximum rate =1800 *veh/hr*, Minimum rate = 400 *veh/hr*

Table 13 Lawrenceville Hwy Ramp Metering

Rate (veh/hr)	Density (veh/km/ln)
1800	5 or less
1800	6
1800	7
1800	8
1800	9
1800	10
1800	11
1600	12
1450	13
1300	14
1150	15
1000	16
850	17
700	18
550	19
400	20 or more

5.3.8. Church St.

K_R=86, Critical Density = 25 (*veh/km/lane*), Maximum rate =1800 *veh/hr*, Minimum rate = 400 *veh/hr*

Table 14 Church St. Ramp Metering

Rate (veh/hr)	Density (veh/km/ln)
1800	10 or less
1800	11
1700	12
1600	13
1500	14
1400	15
1300	16
1200	17
1100	18
1000	19
900	20
800	21
700	22
600	23
500	24
400	25 or more

5.3.9. Memorial Drive

K_R=97, Critical Density = 25 (*veh/km/lane*), Maximum rate =1800 *veh/hr*, Minimum rate = 400 *veh/hr*

Table 15 Memorial Drive Ramp Metering

Rate (veh/hr)	Density (veh/km/ln)
1800	10 or less
1800	11
1700	12
1600	13
1500	14
1400	15
1300	16
1200	17
1100	18
1000	19
900	20
800	21
700	22
600	23
500	24
400	25 or more

5.3.10. Covington Hwy

K_R=155, Critical Density = 25 (*veh/km/lane*), Maximum rate =1800 *veh/hr*, Minimum rate = 400 *veh/hr*

Table 16 Covington Hwy Ramp Metering

Rate (veh/hr)	Density (veh/km/ln)
1800	10 or less
1800	11
1800	12
1800	13
1800	14
1800	15
1750	16
1600	17
1450	18
1300	19
1150	20
1000	21
850	22
700	23
550	24
400	25 or more

5.3.11. Glenwood Rd

K_R=94, Critical Density = 23 (*veh/km/lane*), Maximum rate =1800 *veh/hr*, Minimum rate = 400 *veh/hr*

Table 17 Glenwood Rd Ramp Metering

Rate (veh/hr)	Density (veh/km/ln)
1800	10 or less
1600	11
1500	12
1100	13
1300	14
1200	15
1100	16
1000	17
900	18
800	19
700	20
600	21
500	22
400	23 or more

6. Conclusions

This study used a simulation based optimization framework to determine optimal parameter values of GDOT's *MaxView* ramp-metering system to minimize the total travel time in the study corridor. As a part of this framework, the microsimulation model (GTsim) and a GA based optimization module were integrated. The optimal values derived from this study were found to reduce travel times by more than 4.5% compared to no-metering scenario. These savings are not trivial considering that the upstream sections of corridor (near Peachtree Industrial Blvd and North Peachtree Rd) gets completely congested by the end of the congestion period. Considering that many ramps of the study corridor operate at minimum rate after certain time, it can be stated that most of the benefits of parameter optimization is realized during the congestion build-up phase.

From the optimal parameter values and the critical density downstream of the ramp metering that are derived in this study, we generated optimal metering rates for each location of the study corridor, which can be readily implemented in GDOT's MaxView ramp metering system. Notice that these metering rates are approximations of our results that can be implemented in the current system, which does not have the capabilities of implementing real-time control such as ALINEA. However, the new version of MaxView that is about to be implemented by GDOT, will have the ability to directly implement the results of our study.

This page is intentionally left blank.

7. References

Banks, J. H. (1993). Effect of response limitations on traffic-responsive ramp metering. *Transportation Research Record*, (1394).

Bogenberger, K., Vukanovic, S., & Keller, H. (2002). ACCEZZ—Adaptive Fuzzy Algorithms for Traffic Responsive and Coordinated Ramp Metering. In *Journal of Transportation Engineering* (Vol. 49, pp. 744–753). ASCE.

Chilukuri, B. R., Laval, J. A., & Guin, A. (2014). MicroSimulation-Based Framework for Freeway Travel Time Forecasting. *Transportation Research Record: Journal of the Transportation Research Board*, *2470*, 34–45.

Diakaki, C., & Papageorgiou, M. (1994). *Design and Simulation Test of Coordinated Ramp Metering Control (METALINE) for A10-West in Amsterdam. Internal Report No. 1994-2*. ATT-Project Eurocor V2017.

Guin, A., & Laval, J. (2013). *Development of Optimal Ramp Metering Strategies Final Report (GDOT Research Project TO 02-98; RSCH PROJ 11-18 Georgia Tech Project No. 2006S18)*.

Iida Y., Hasegawa T., Asakura Y., S. C. F. (1989). A formulation of on-ramp traffic control system with route guidance for urban expressway. In *IFAC/IFFIP/IFORS/-Sixth International Conference on Control in Transportation Systems* (pp. 229–236).

Jacobson, L., Henry, K., & Mehyar, O. (1989). Real-time metering algorithm for centralized control. *Transportation Research Record*, (1732), 20–32.

Jacobson, L., Stribiak, J., Nelson, L., & Sallman, D. (2006). *Ramp Management and*

Control Handbook.

Lasdon, L. S., Fox, R. L., & Ratner, M. W. (1974). Nonlinear optimization using the generalized reduced gradient method. *RAIRO Operations Research, 8*, 73–103.

Lipp, L. E., Corcoran, L. J., & Hickman, G. A. (1991). Benefits of central computer control for Denver ramp-metering system. *Transportation Research Record*, (1320).

Liu, H. X., Wu, X., & Michalopoulos, P. G. (2007). Improving Queue Size Estimation for Minnesota's Stratified Zone Metering Strategy. *Transportation Research Record, 2012*(1), 38–46. https://doi.org/10.3141/2012-05

Masher, D. P., Ross, D. W., Wong, P. J., Tuan, P. L., Zeidler, H. M., & Peracek, S. (1975). *Guidelines for design and operating of ramp control systems. SRI, Menid Park, CA, Stanford Res. Inst. Rep. NCHRP 3-22, SRI Project 3340.* Menlo Park, California.

Paesani, G., Kerr, J., Perovich, P., & Khosravi, F. E. (1997). System wide adaptive ramp metering (SWARM). *Merging the Transportation and Communications Revolutions. Abstracts for ITS America Seventh Annual Meeting and Exposition*.

Papageorgiou, M. (1980). A new approach to time-of-day control based on a dynamic freeway traffic model. *Transportation Research Part B: Methodological*, *14*(4), 349–360. https://doi.org/10.1016/0191-2615(80)90015-6

Papageorgiou, M., Blosseville, J.-M., & Haj-Salem, H. (1990). Modelling and real-time control of traffic flow on the southern part of Boulevard Peripherique in Paris: Part II: Coordinated on-ramp metering. *Transportation Research Part A: General*, *24*(5),

361–370. https://doi.org/10.1016/0191-2607(90)90048-B

Papageorgiou, M., Hadj-Salem, H., & Blosseville, J. M. (1991). Alinea. A local feedback control law for on-ramp metering. *Transportation Research Record: Journal of the Transportation Research Board*, *1320*, 58–64. https://doi.org/10.1002/cncr.11316

Papageorgiou, M., Hadj-Salem, H., & Middelham, F. (1997). ALINEA Local Ramp Metering: Summary of Field Results. *Transportation Research Record*, *1603*(1), 90–98. https://doi.org/10.3141/1603-12

Papageorgiou, M., Jean-marc, B., & Hadj-salem, H. (1989). Macroscopic Modelling of traffic flow on the Boulevard Peripherique in Paris. *Trafnsportation Research PartB :Methodological*, *236*(ii), 29–47. https://doi.org/10.1016/0191-2615(89)90021-0

Papageorgiou, M., Kosmatopoulos, E., Papamichail, I., & Wang, Y. (2008). A Misapplication of the Local Ramp Metering Strategy ALINEA. *IEEE Transactions on Intelligent Transportation Systems*, *9*(2), 360–364.

Smaragdis, E., & Papageorgiou, M. (2003). Series of New Local Ramp Metering Strategies. *Transportation Research Record: Journal of the Transportation Research Board*, *1856*, 74–86. https://doi.org/10.3141/1856-08

Smaragdis, E., Papageorgiou, M., & Kosmatopoulos, E. (2004). A flow-maximizing adaptive local ramp metering strategy. *Transportation Research Part B*, *38*(3), 251–270.

Stephanedes, Y. J. (1994). Implementation of on-line Zone Control Strategies for optimal

ramp metering in the Minneapolis Ring Road. In *Road Traffic Monitoring and Control, 1994., Seventh International Conference on* (pp. 181–184).

Taylor, C., Meldrum, D., & Jacobson, L. (1998). Fuzzy ramp metering: design overview and simulation results. *Transportation Research Record: Journal of the Transportation Research Board*, *1634*(1), 10–18.

Wang, Y., Kosmatopoulos, E. B., Papageorgiou, M., & Papamichail, I. (2014). Local Ramp Metering in the Presence of a Distant Downstream Bottleneck: Theoretical Analysis and Simulation Study. *IEEE Transactions on Intelligent Transportation Systems*, *15*(5), 2024–2039. https://doi.org/10.1109/TITS.2014.2307884

Wattleworth, J. a. (1965). Peak-period analysis and control of a freeway system. *Highway Research Record*, (89), 1–25.

Yuan L.S. and Kreer, J. B. (1968). An optimal control algorithm for ramp metering of urban freeways. In *6th Annual Allerton Conference on Circuit and System Theory*.

Zhang, H. M., & Ritchie, S. (1997). Freeway ramp metering using artificial neural networks. *Transportation Research Part C: Emerging …*, *5*(5), 273–286.

8. Appendix

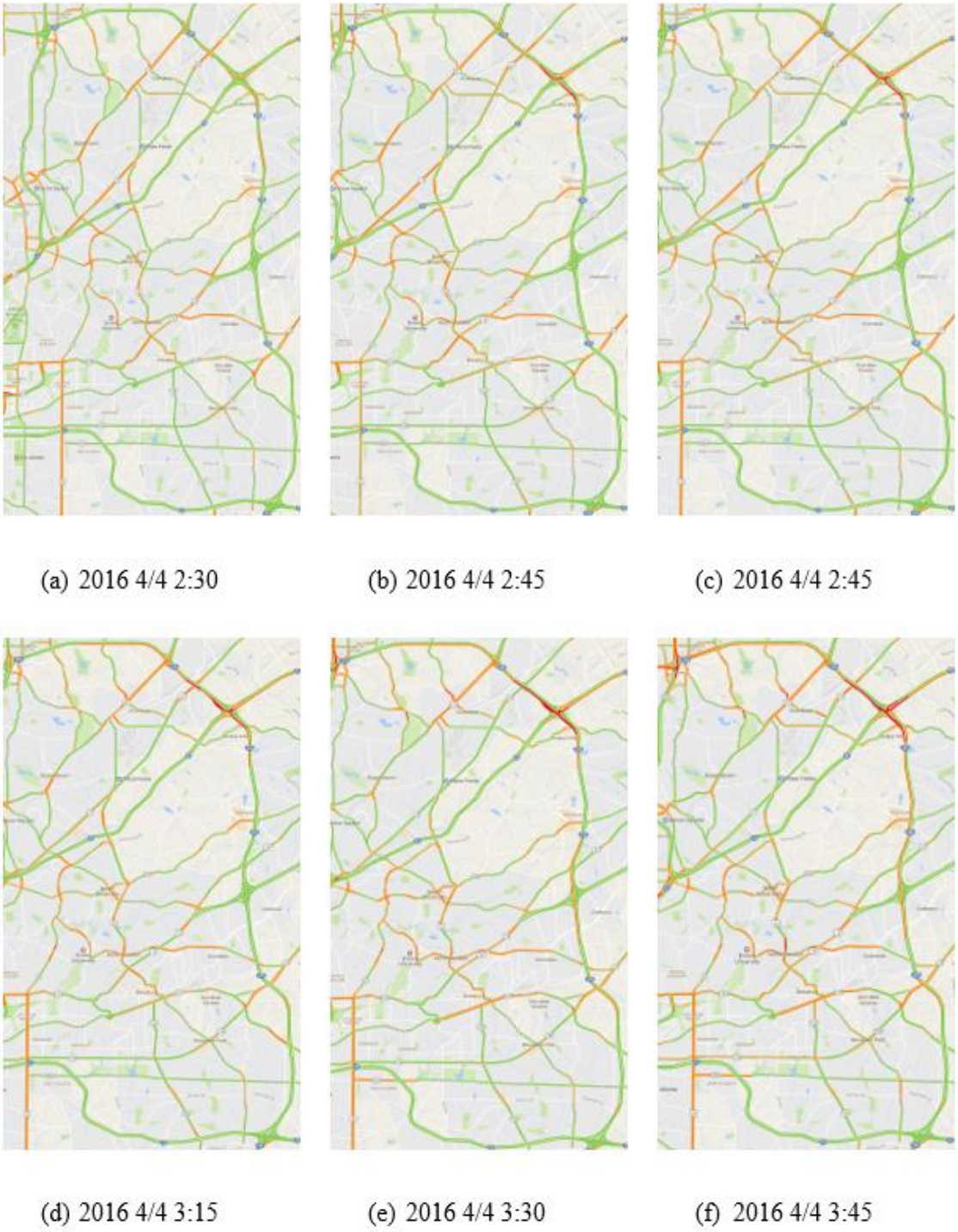

(a) 2016 4/4 2:30 (b) 2016 4/4 2:45 (c) 2016 4/4 2:45

(d) 2016 4/4 3:15 (e) 2016 4/4 3:30 (f) 2016 4/4 3:45

Figure 15 Typical Traffic State on I-285 Corridor on Monday PM Peak

(a) 2016 4/5 2:30 (b) 2016 4/5 2:45 (c) 2016 4/5 2:45

(d) 2016 4/5 3:15 (e) 2016 4/5 3:30 (f) 2016 4/5 3:45

Figure 16 Typical Traffic State on I-285 Corridor on Tuesday PM Peak

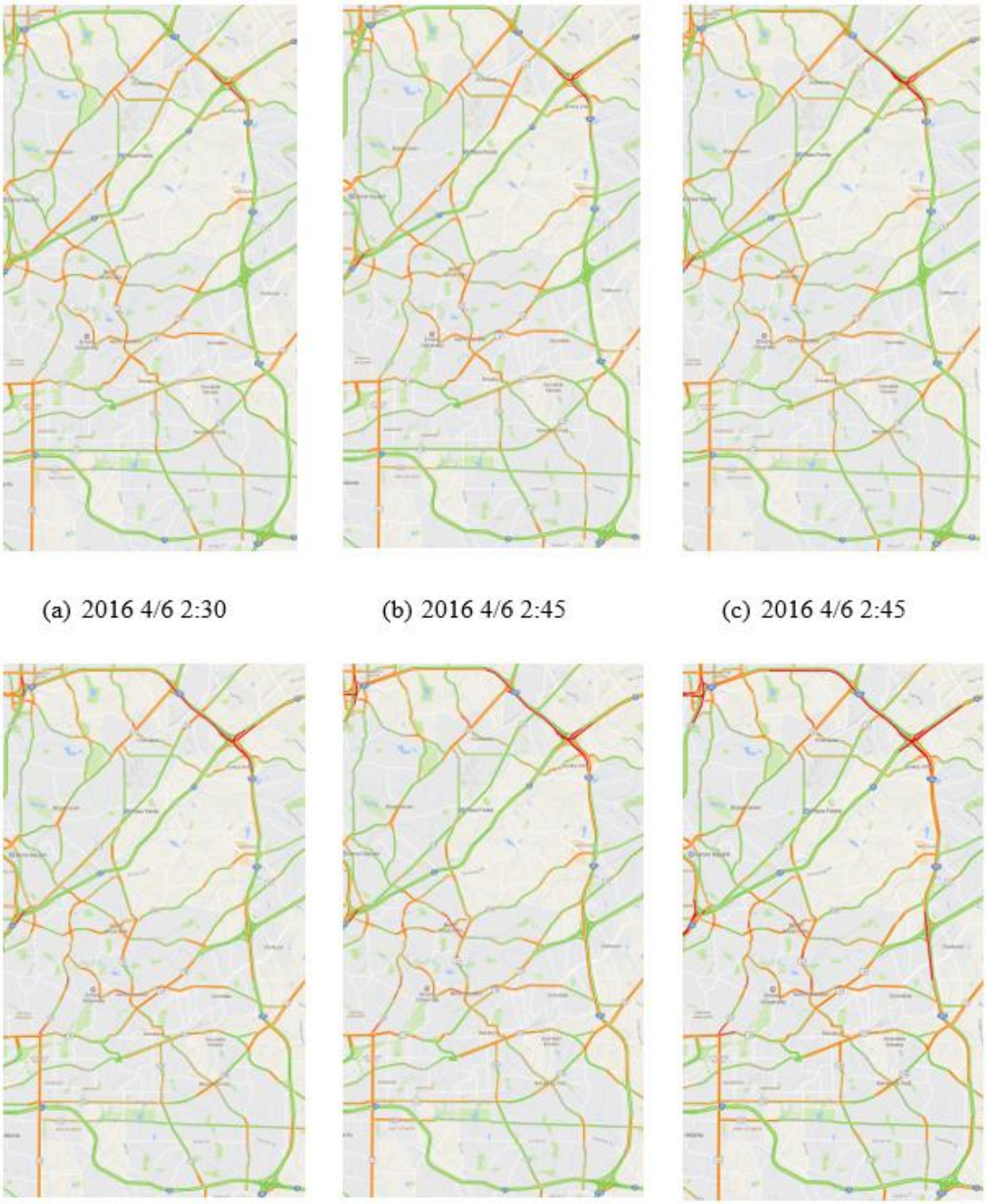

(a) 2016 4/6 2:30 (b) 2016 4/6 2:45 (c) 2016 4/6 2:45

(d) 2016 4/6 3:15 (e) 2016 4/6 3:30 (f) 2016 4/6 3:45

Figure 17 Typical Traffic State on I-285 Corridor on Wednesday PM Peak

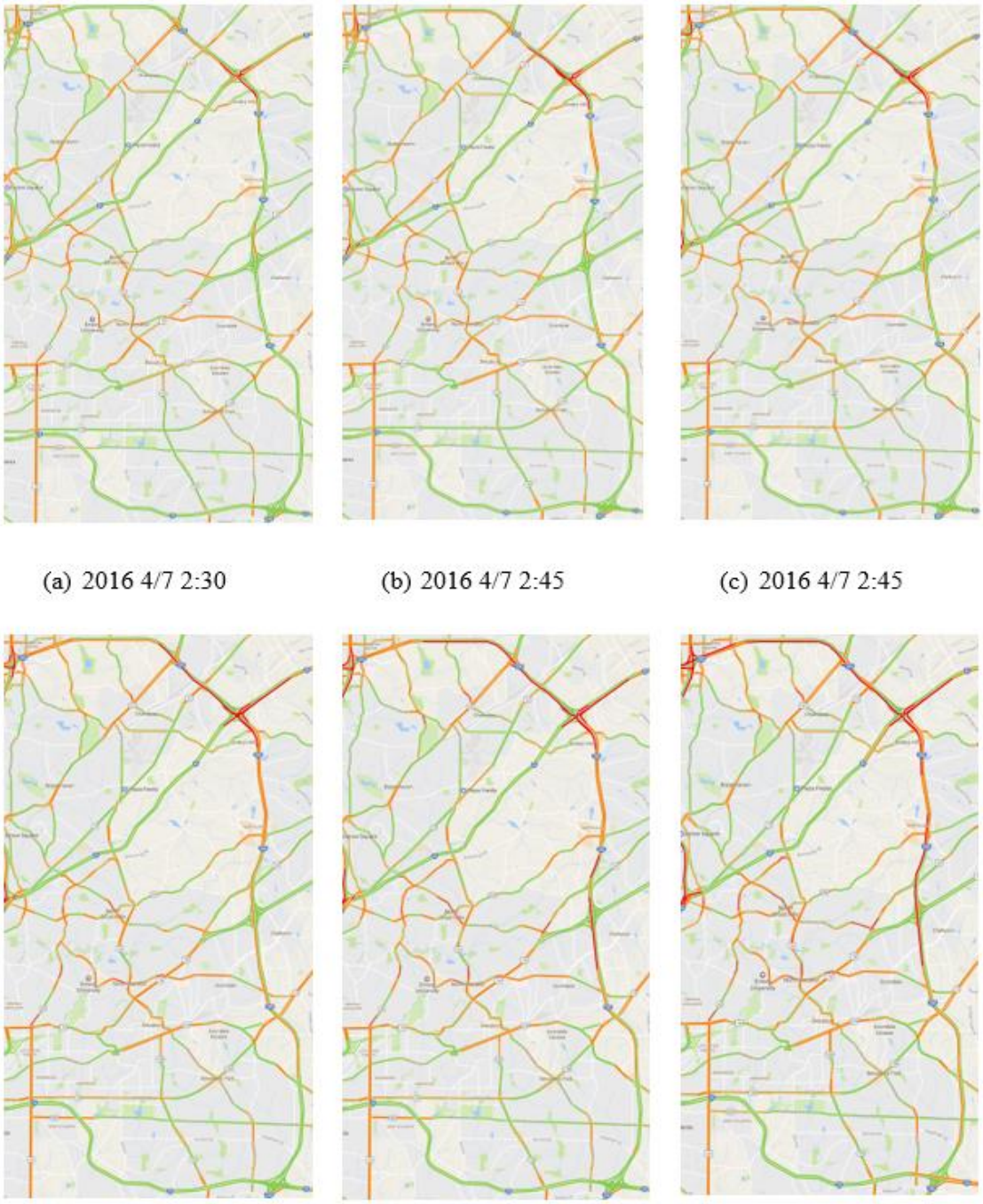

(a) 2016 4/7 2:30 (b) 2016 4/7 2:45 (c) 2016 4/7 2:45

(d) 2016 4/7 3:15 (e) 2016 4/7 3:30 (f) 2016 4/7 3:45

Figure 18 Typical Traffic State on I-285 Corridor on Thursday PM Peak

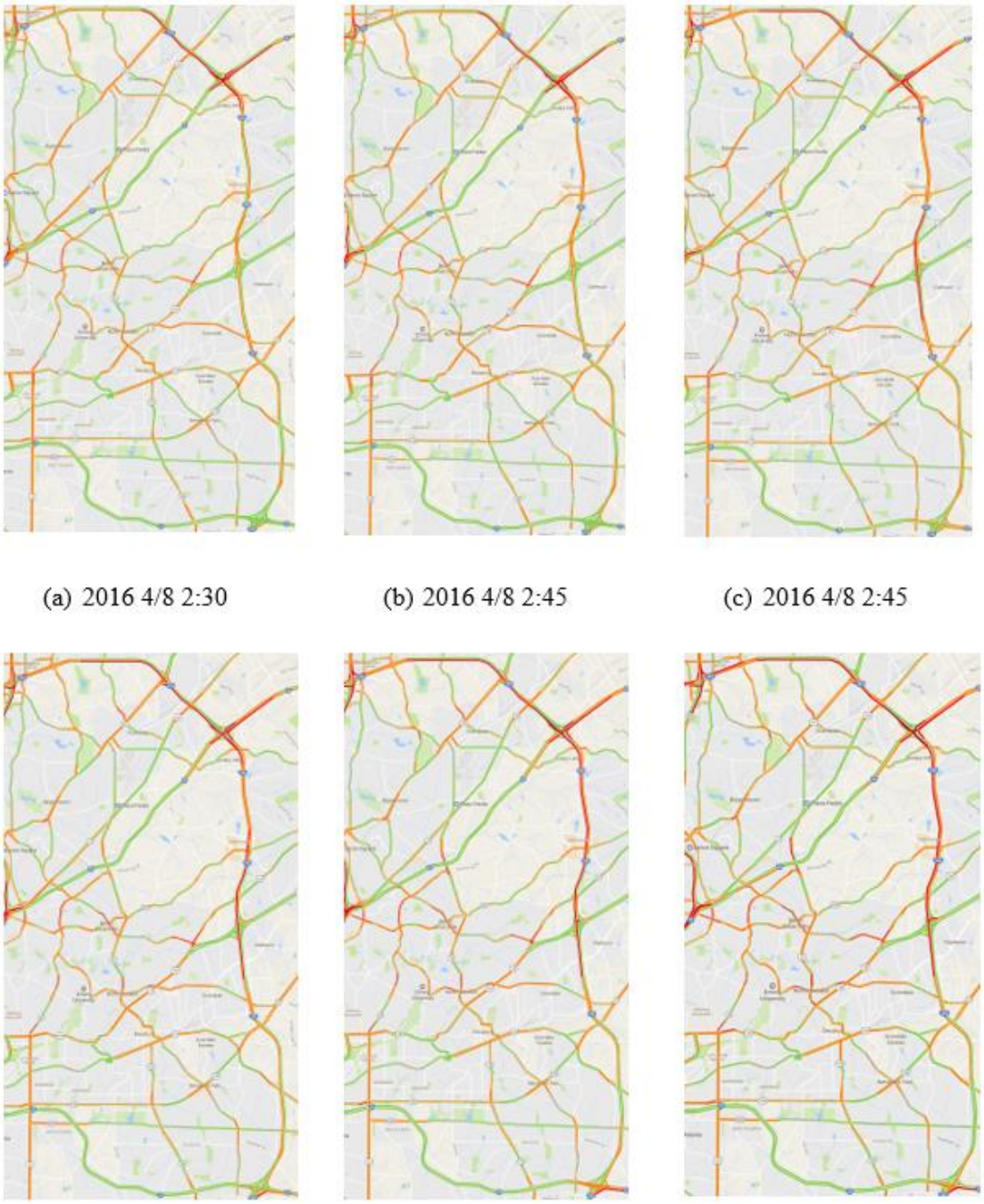

(a) 2016 4/8 2:30 (b) 2016 4/8 2:45 (c) 2016 4/8 2:45

(d) 2016 4/8 3:15 (e) 2016 4/8 3:30 (f) 2016 4/8 3:45

Figure 19 Typical Traffic State on I-285 Corridor on Friday PM Peak

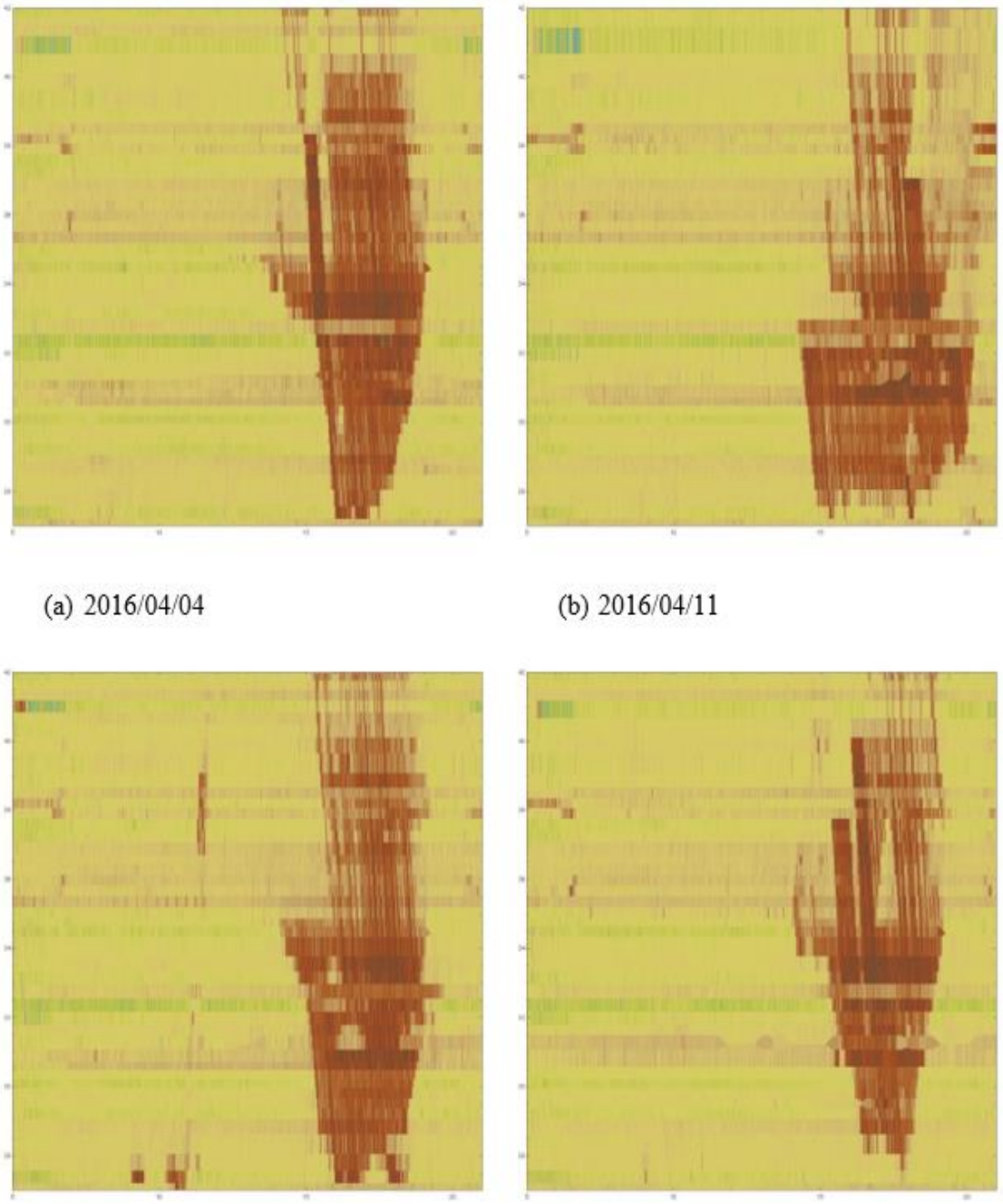

(a) 2016/04/04

(b) 2016/04/11

(c) 2016/04/18

(d) 2016/04/25

Figure 20 April 2016 Monday Traffic. Low-speed regions are in brown and high-speed regions are in yellow.

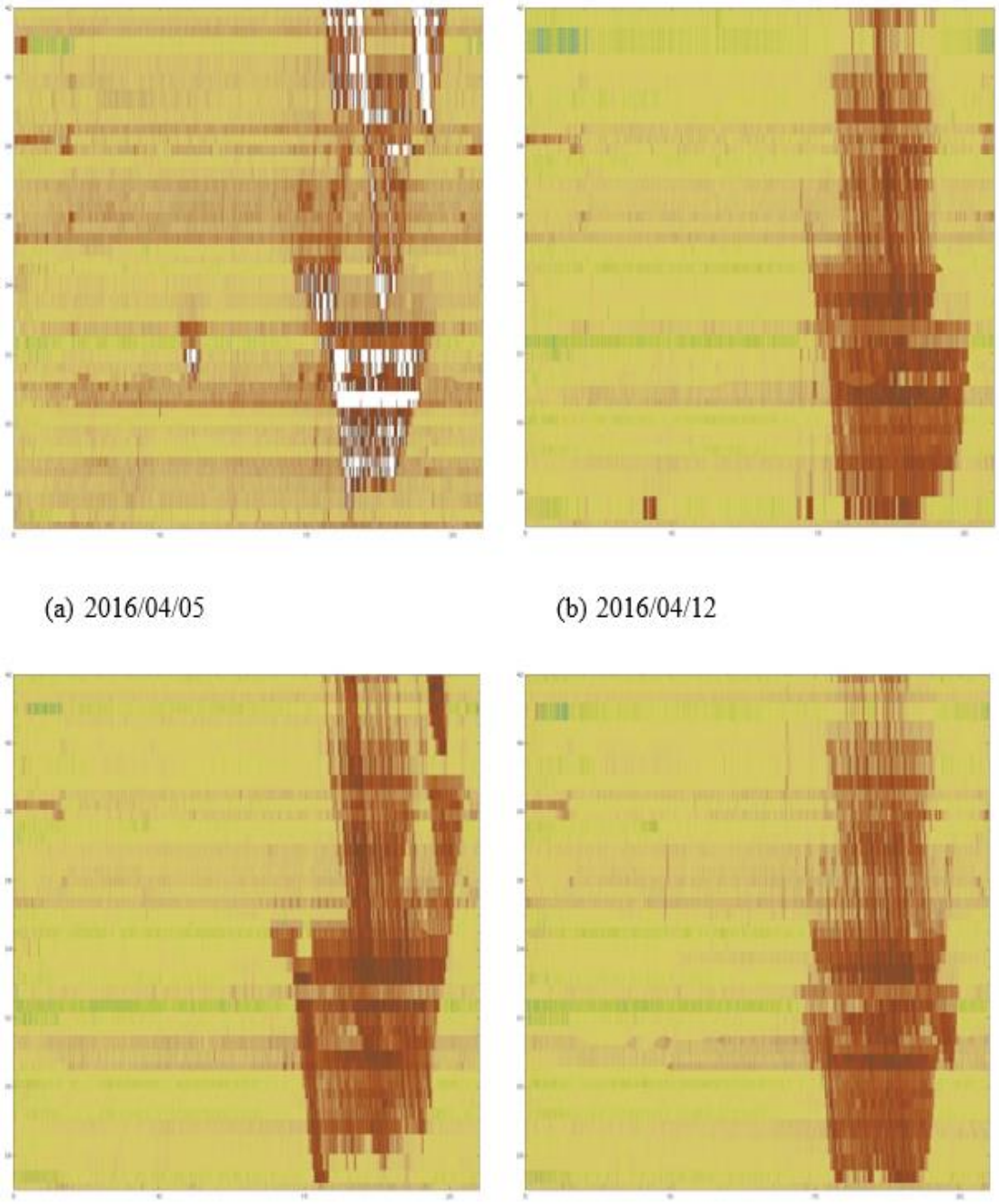

Figure 21 April 2016 Tuesday Traffic. Low-speed regions are in brown and high-speed regions are in yellow.

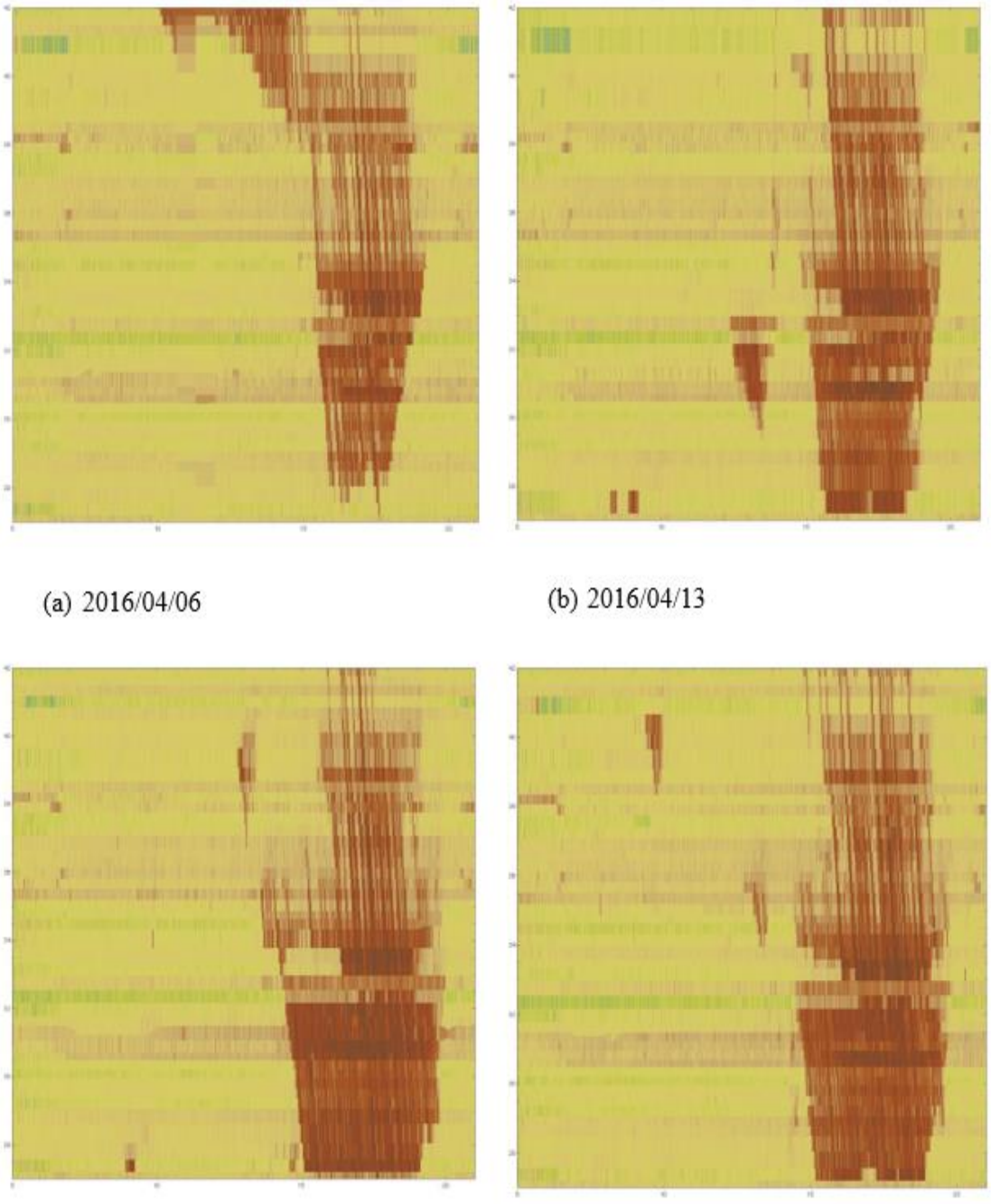

Figure 22 April 2016 Wednesday Traffic. Low-speed regions are in brown and high-speed regions are in yellow.

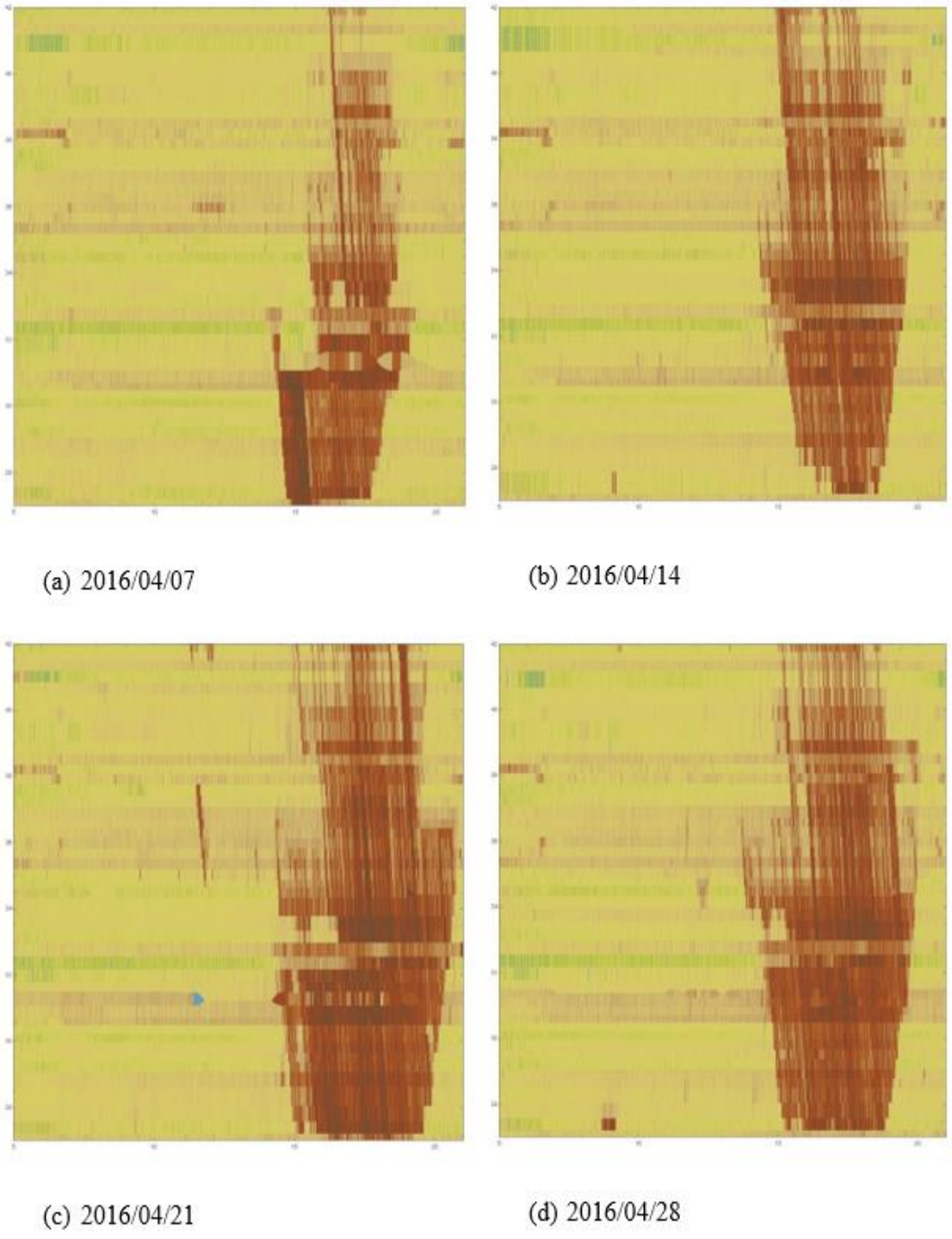

Figure 23 April 2016 Thursday Traffic. Low-speed regions are in brown and high-speed regions are in yellow.

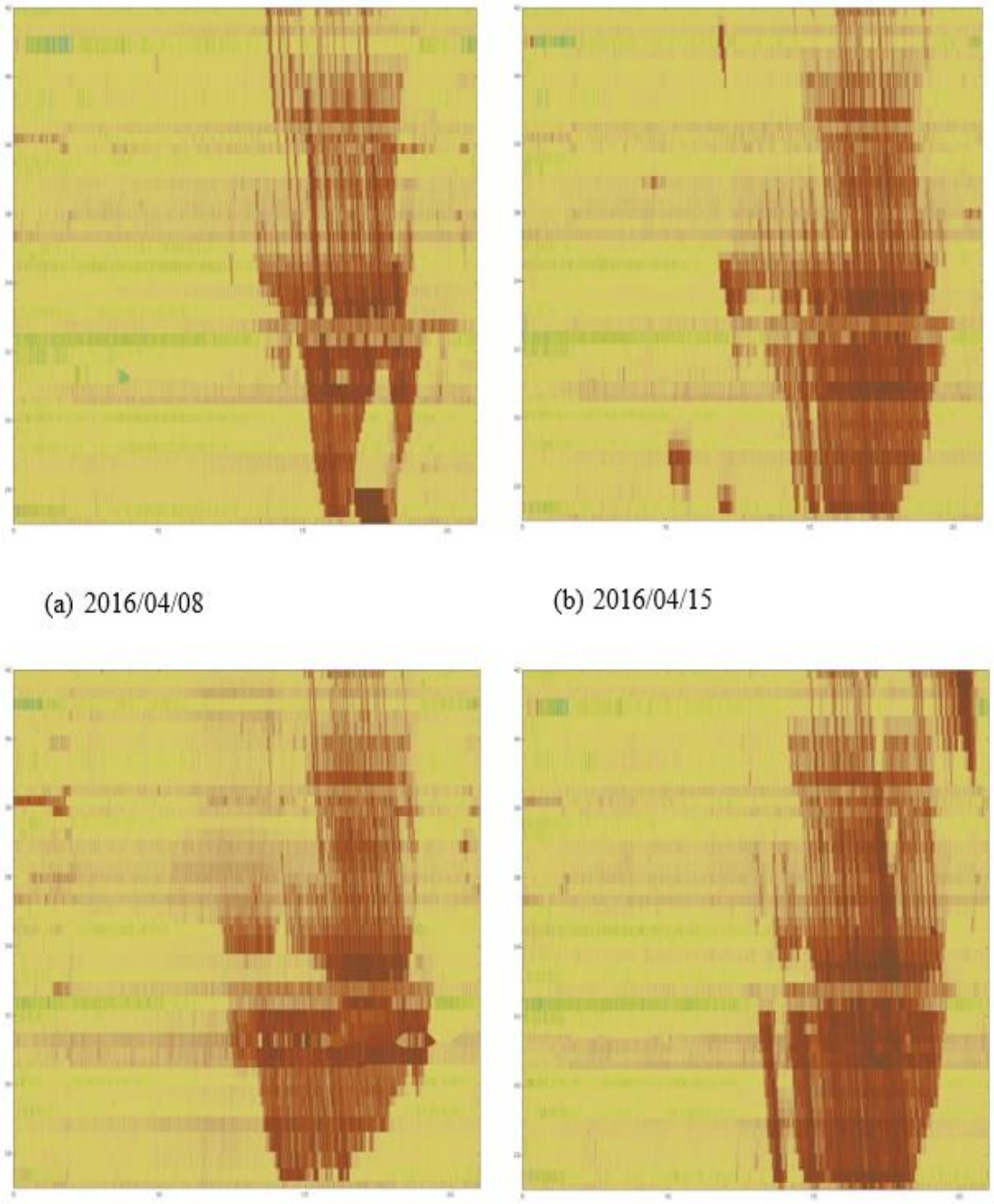

Figure 24 April 2016 Friday Traffic. Low-speed regions are in brown and high-speed regions are in yellow.

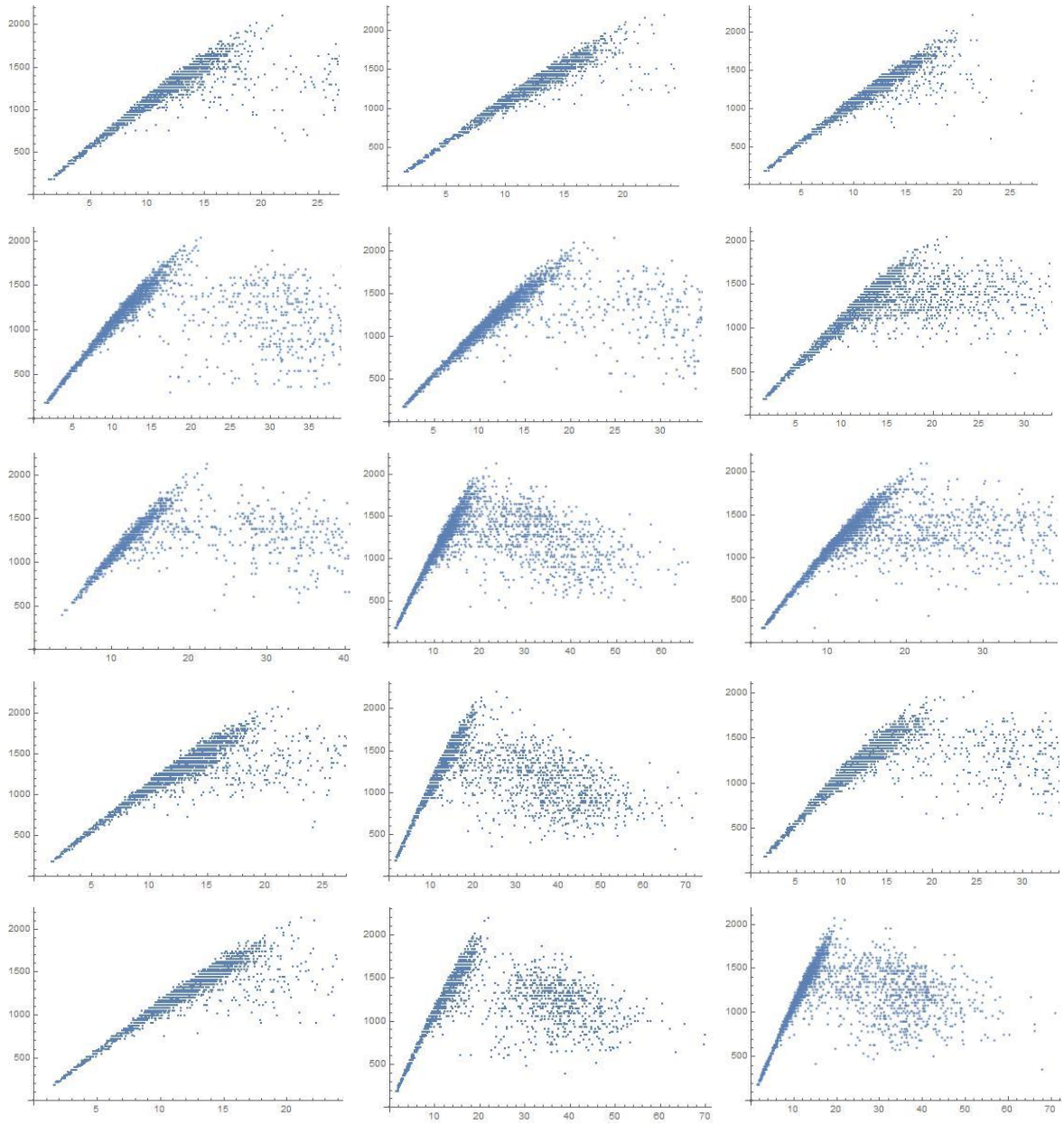

Figure 25 Flow-Occupancy (per lane) curve at D/S of Peachtree Dunwoody Road, April 2016. Flow is in vehicle/hr and occupancy is defined as the percentage of time that the sensor is occupied by a vehicle.

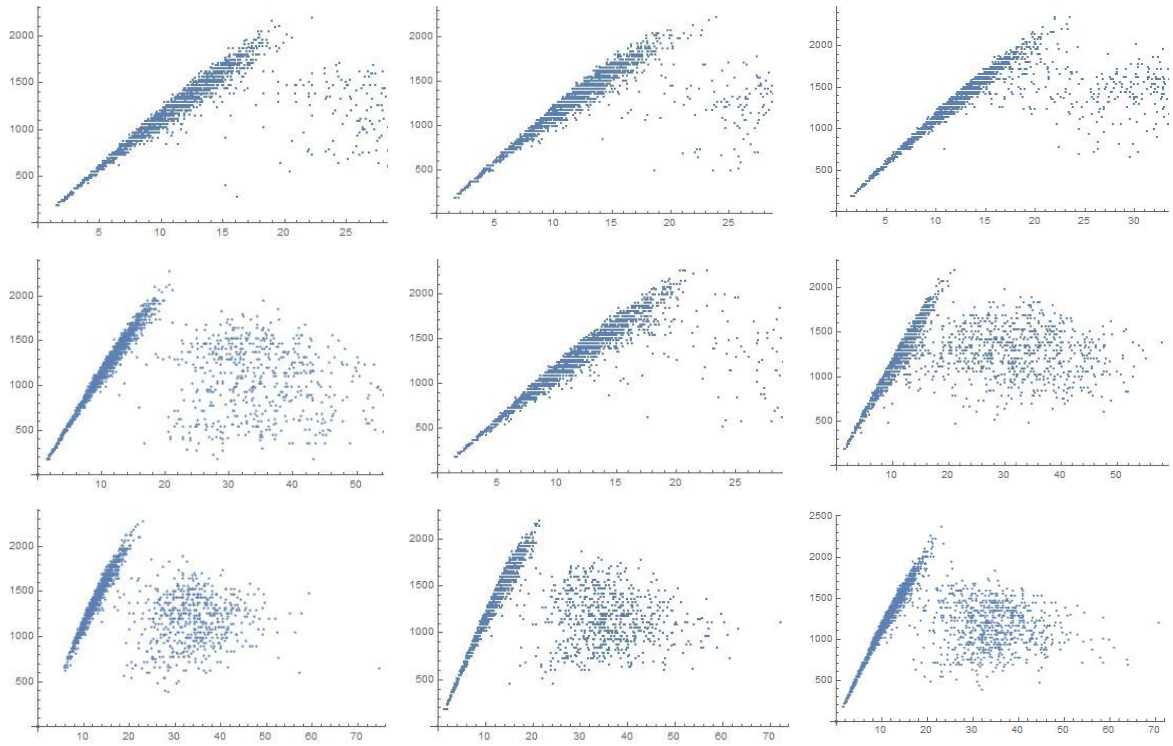

Figure 26 Flow-Occupancy (per lane) curve at D/S of Ashford Dunwoody Road, April 2016. Flow is in vehicle/hr and occupancy is defined as the percentage of time that the sensor is occupied by a vehicle.

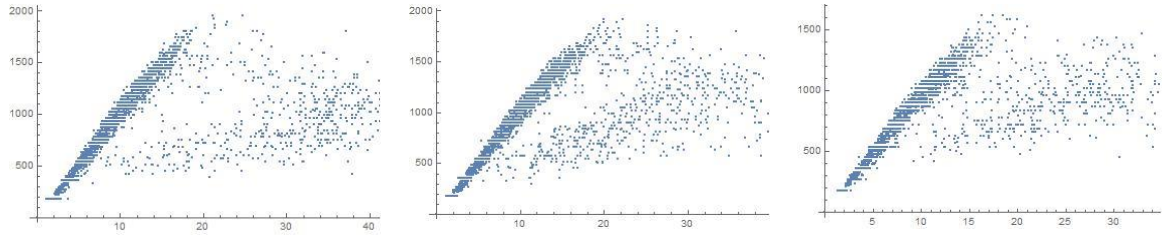

Figure 27 Flow-Occupancy (per lane) curve at D/S of North Peachtree Road, April 2016. Flow is in vehicle/hr and occupancy is defined as the percentage of time that the sensor is occupied by a vehicle.

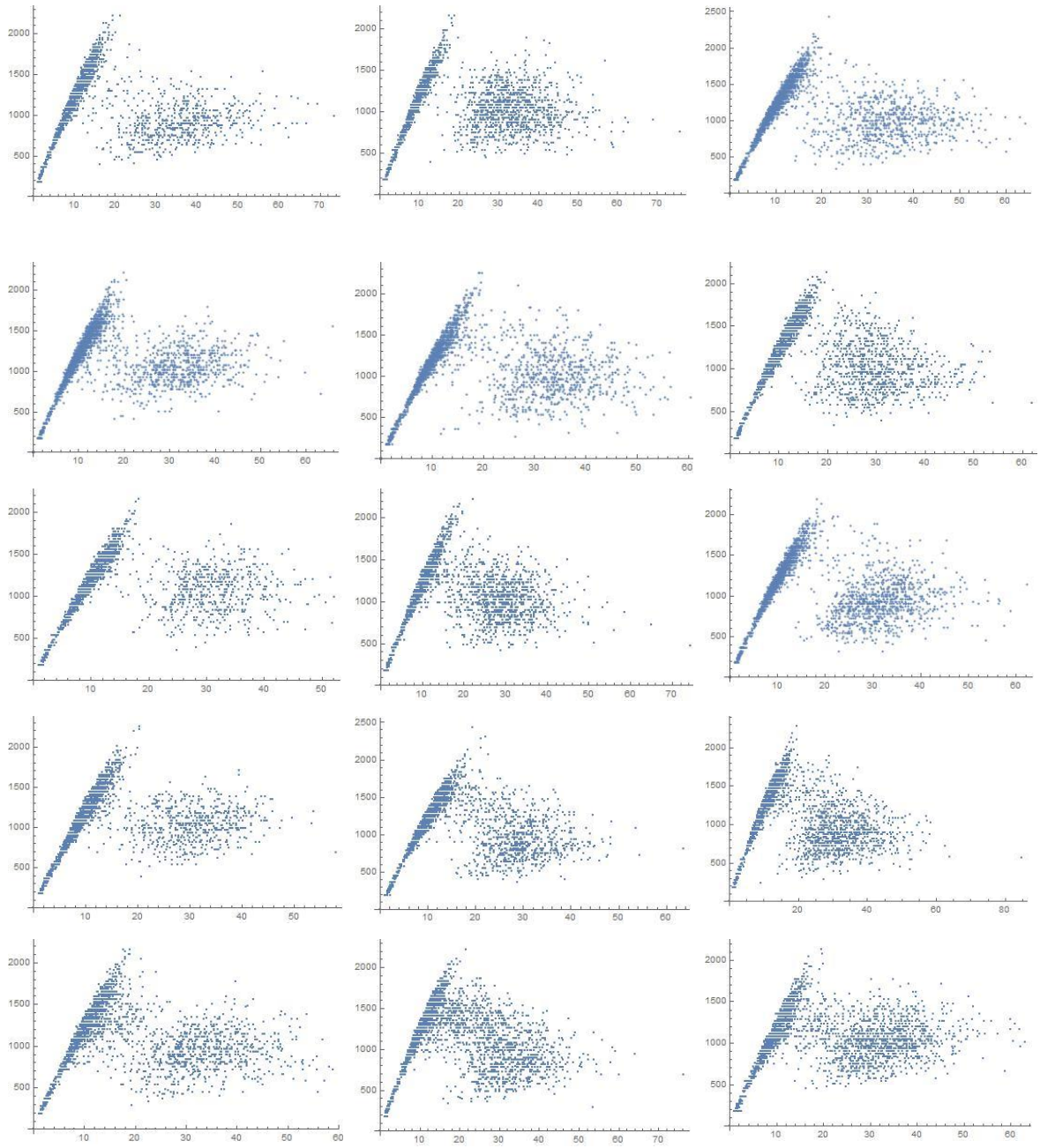

Figure 28 Flow-Occupancy (per lane) curve at D/S of Peachtree Industrial Blvd, April 2016. Flow is in vehicle/hr and occupancy is defined as the percentage of time that the sensor is occupied by a vehicle.

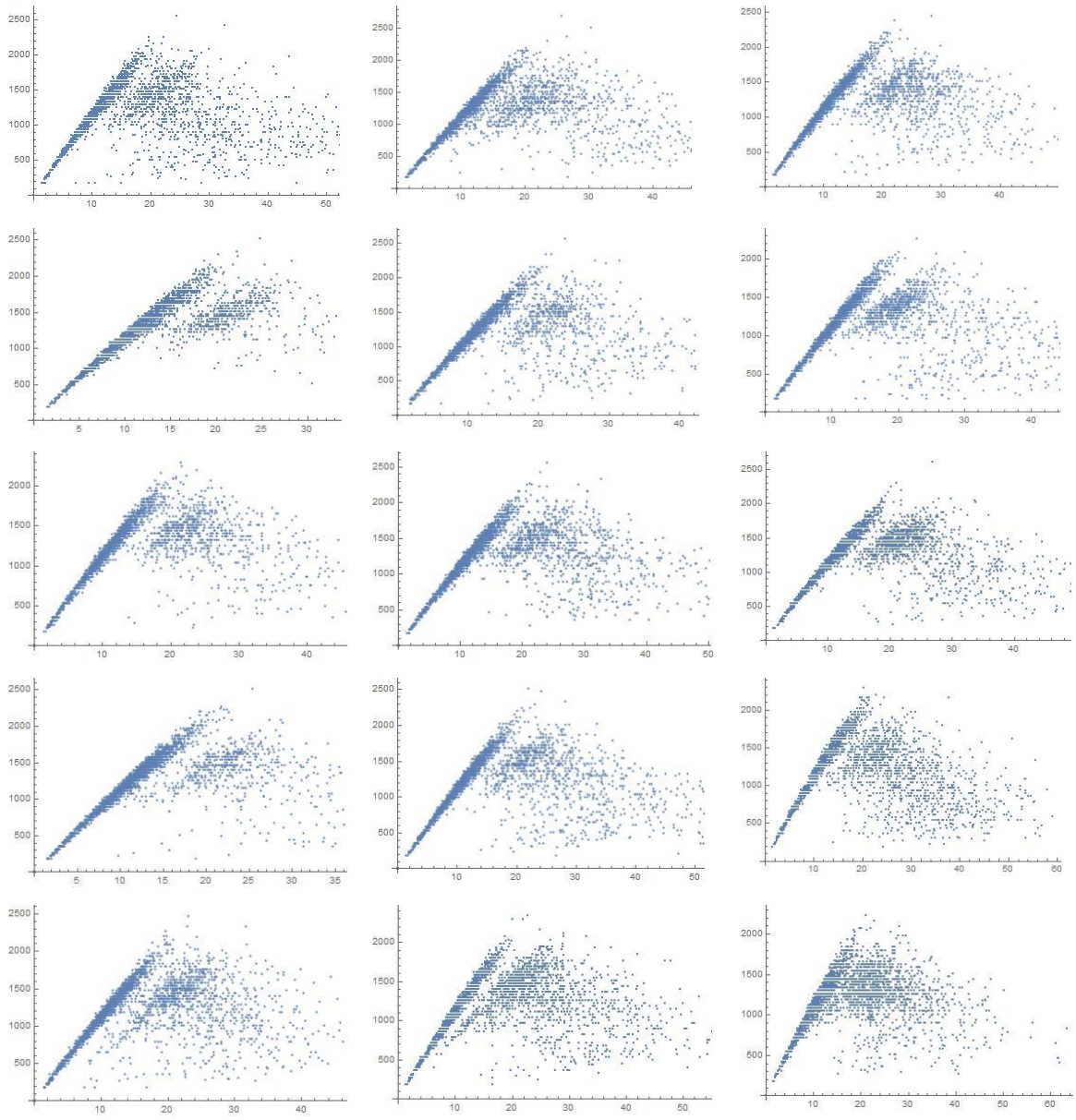

Figure 29 Flow-Occupancy (per lane) curve at D/S of Chamblee Tucker Road, April 2016. Flow is in vehicle/hr and occupancy is defined as the percentage of time that the sensor is occupied by a vehicle.

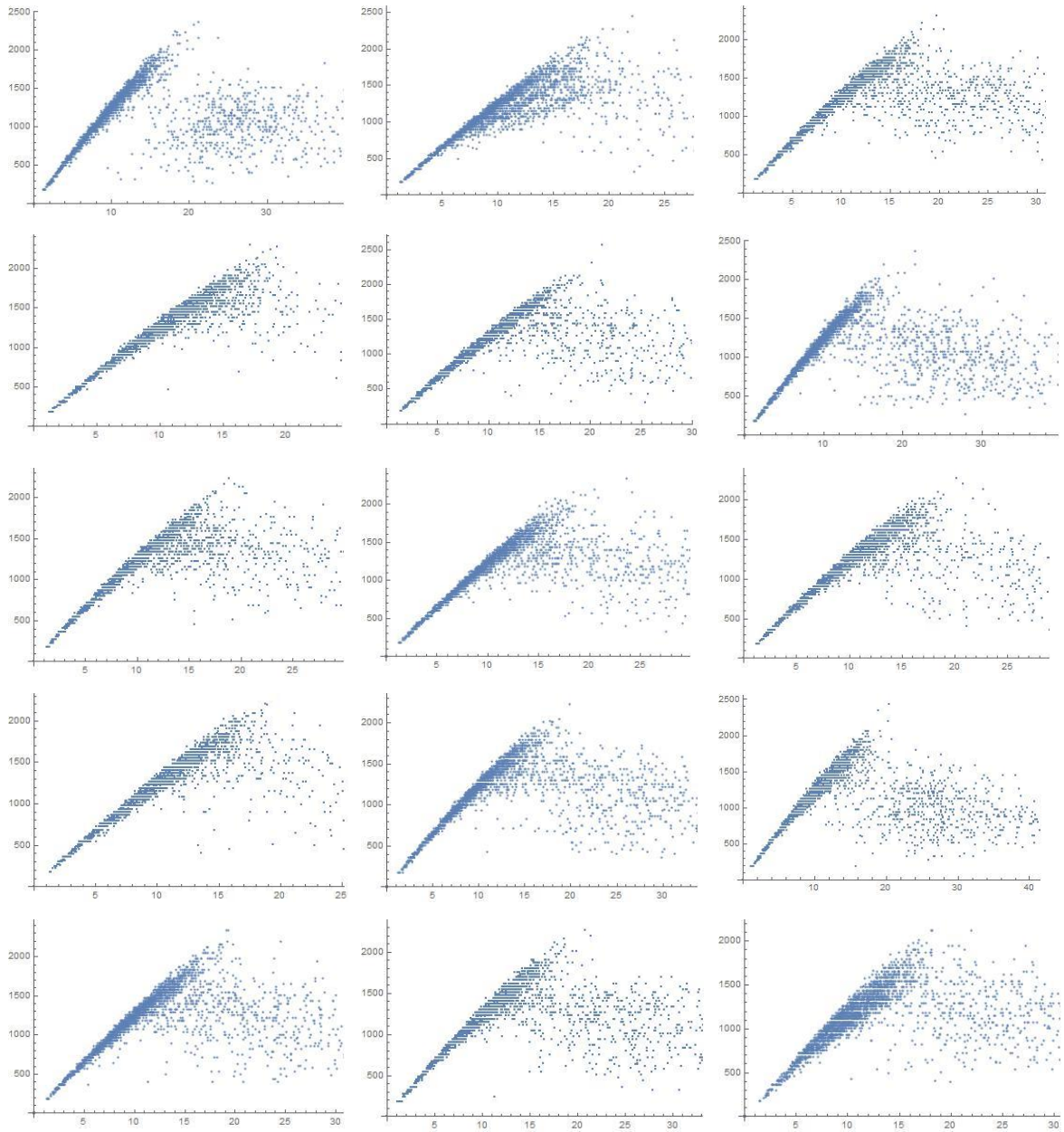

Figure 30 Flow-Occupancy (per lane) curve at D/S of Lavista Road, April 2016. Flow is in vehicle/hr and occupancy is defined as the percentage of time that the sensor is occupied by a vehicle.

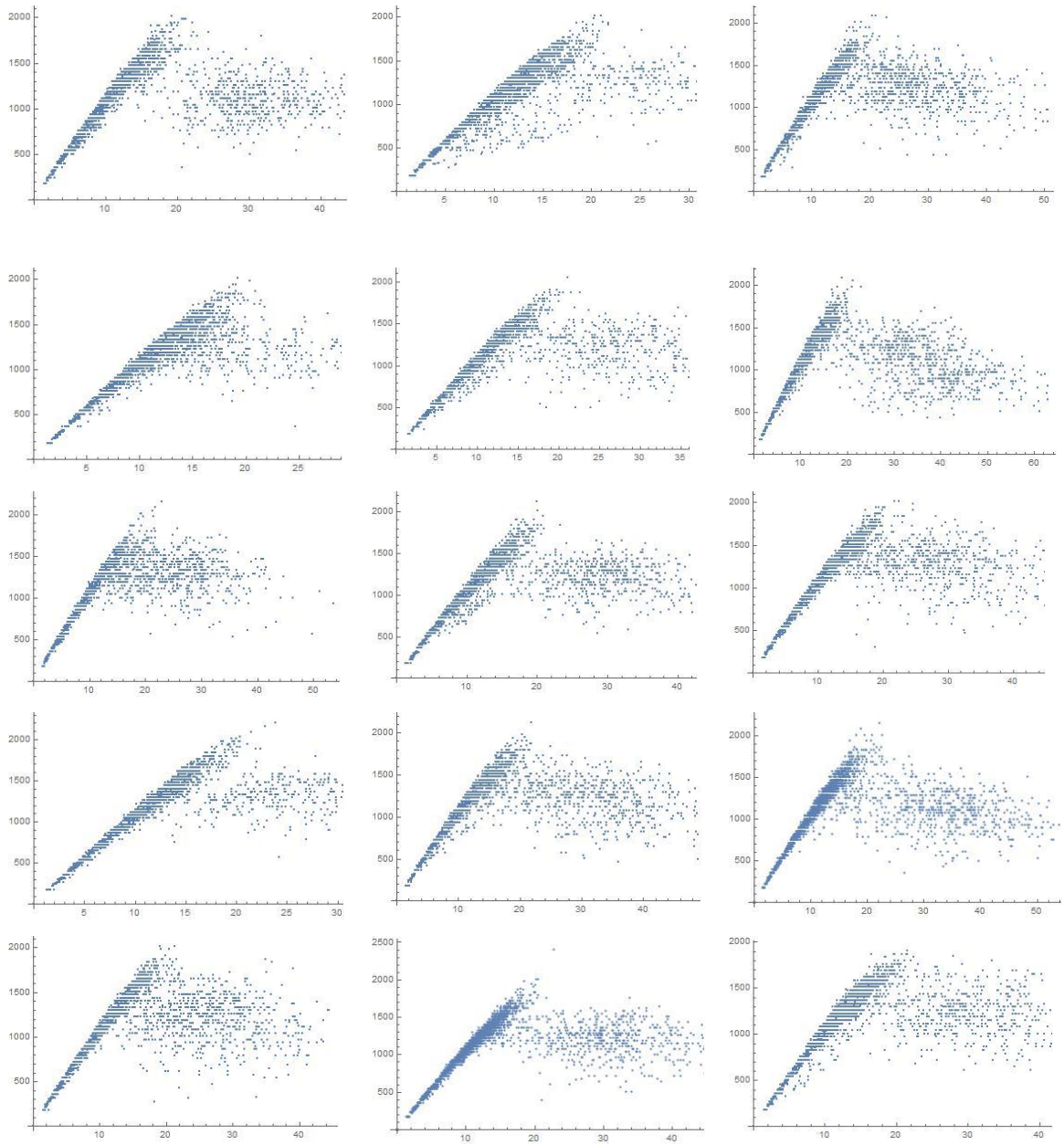

Figure 31 Flow-Occupancy (per lane) curve at D/S of Lawrenceville Hwy, April 2016. Flow is in vehicle/hr and occupancy is defined as the percentage of time that the sensor is occupied by a vehicle.

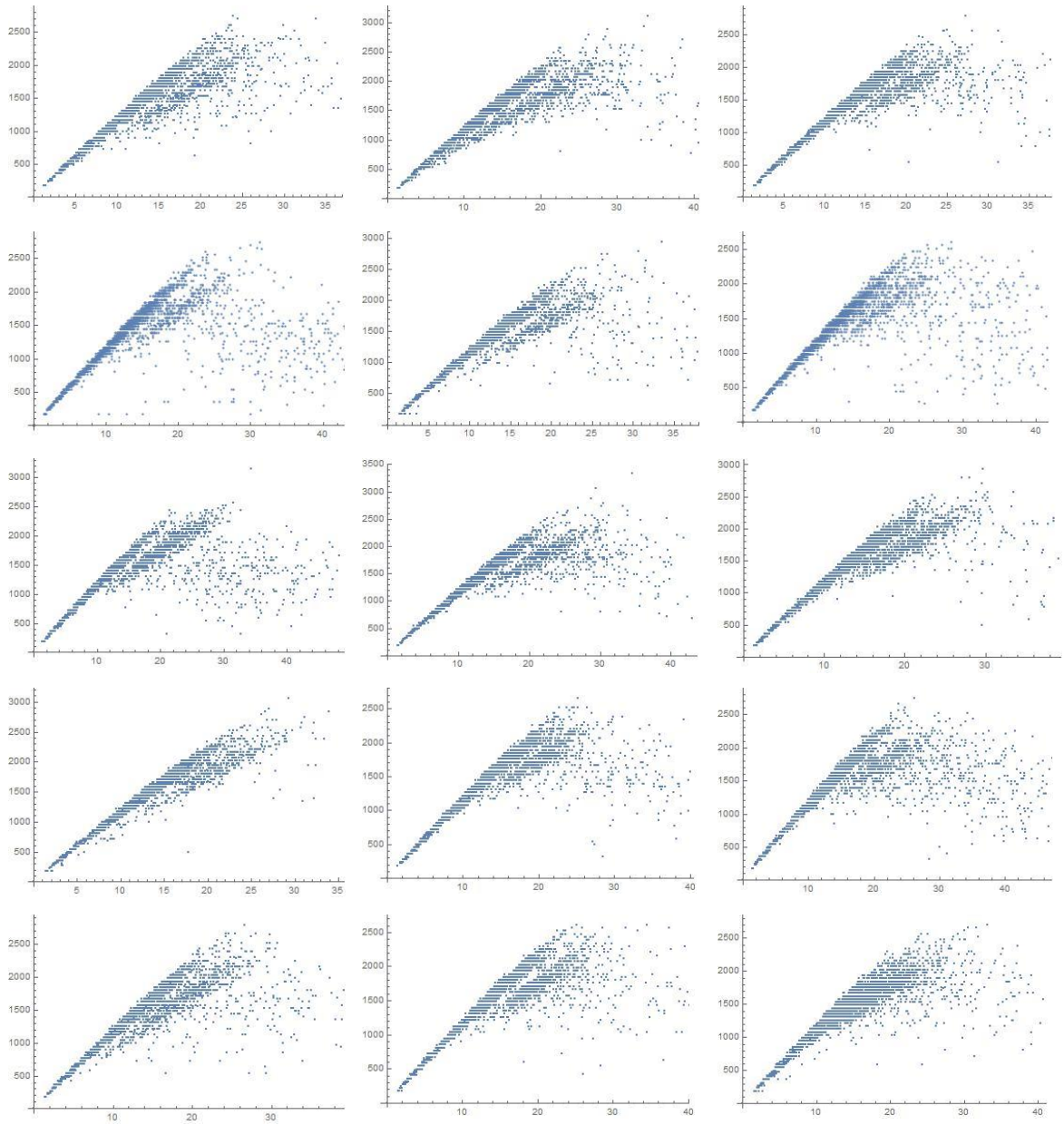

Figure 32 Flow-Occupancy (per lane) curve at D/S of Church Street, April 2016. Flow is in vehicle/hr and occupancy is defined as the percentage of time that the sensor is occupied by a vehicle.

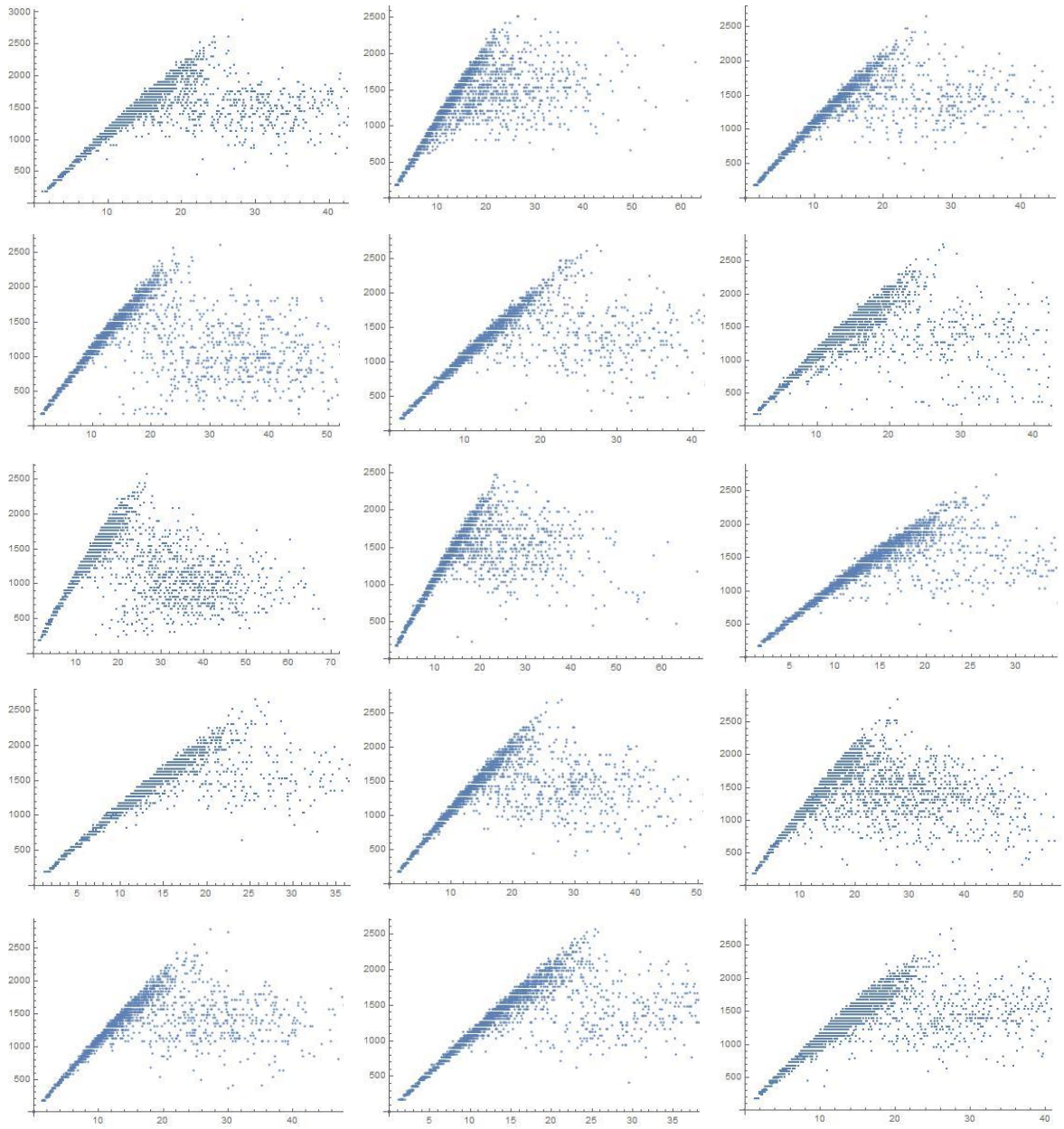

Figure 33 Flow-Occupancy (per lane) curve at D/S of Memorial Drive, April 2016. Flow is in vehicle/hr and occupancy is defined as the percentage of time that the sensor is occupied by a vehicle.

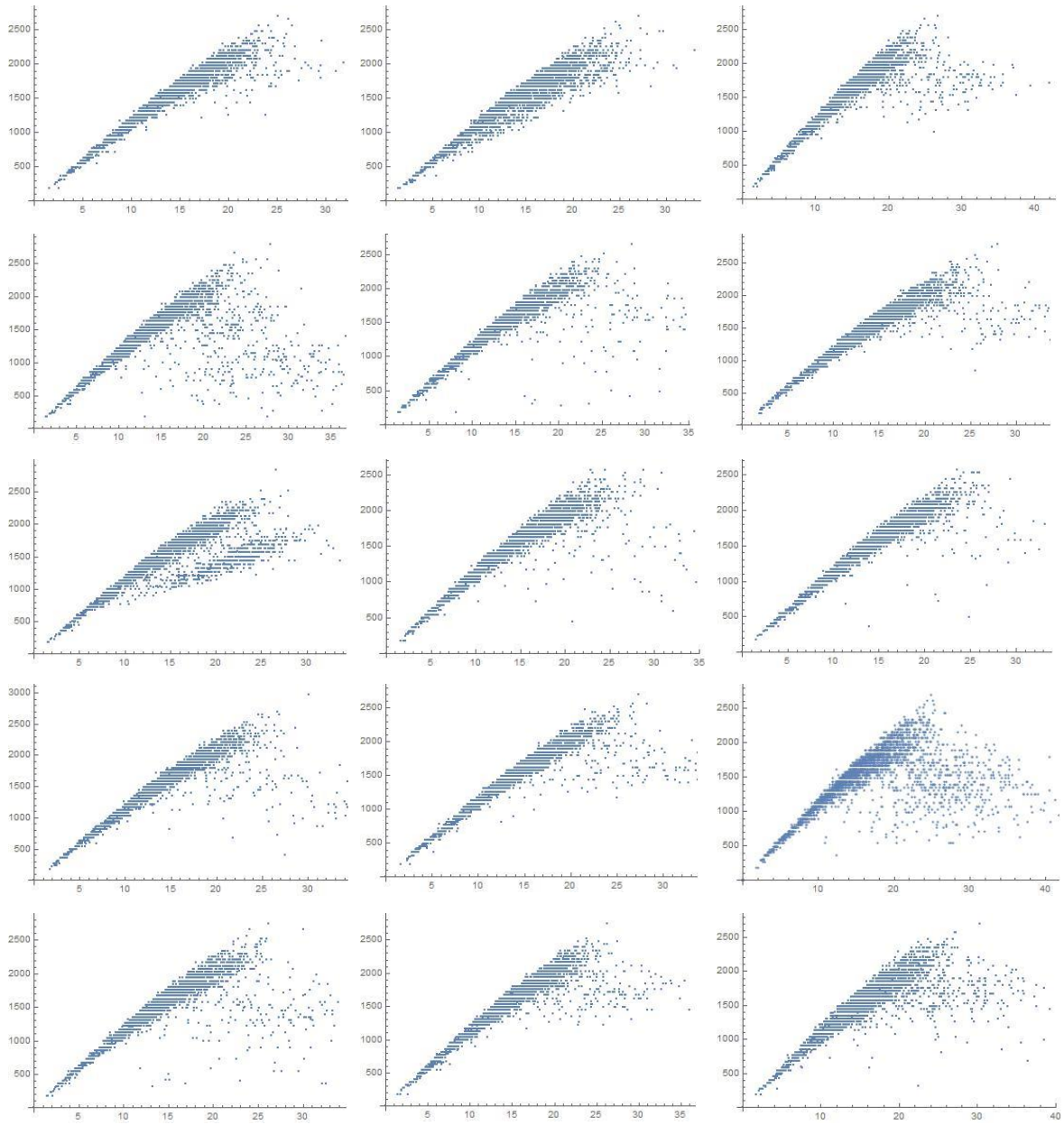

Figure 34 Flow-Occupancy (per lane) curve at D/S of Covington Hwy, April 2016. Flow is in vehicle/hr and occupancy is defined as the percentage of time that the sensor is occupied by a vehicle.

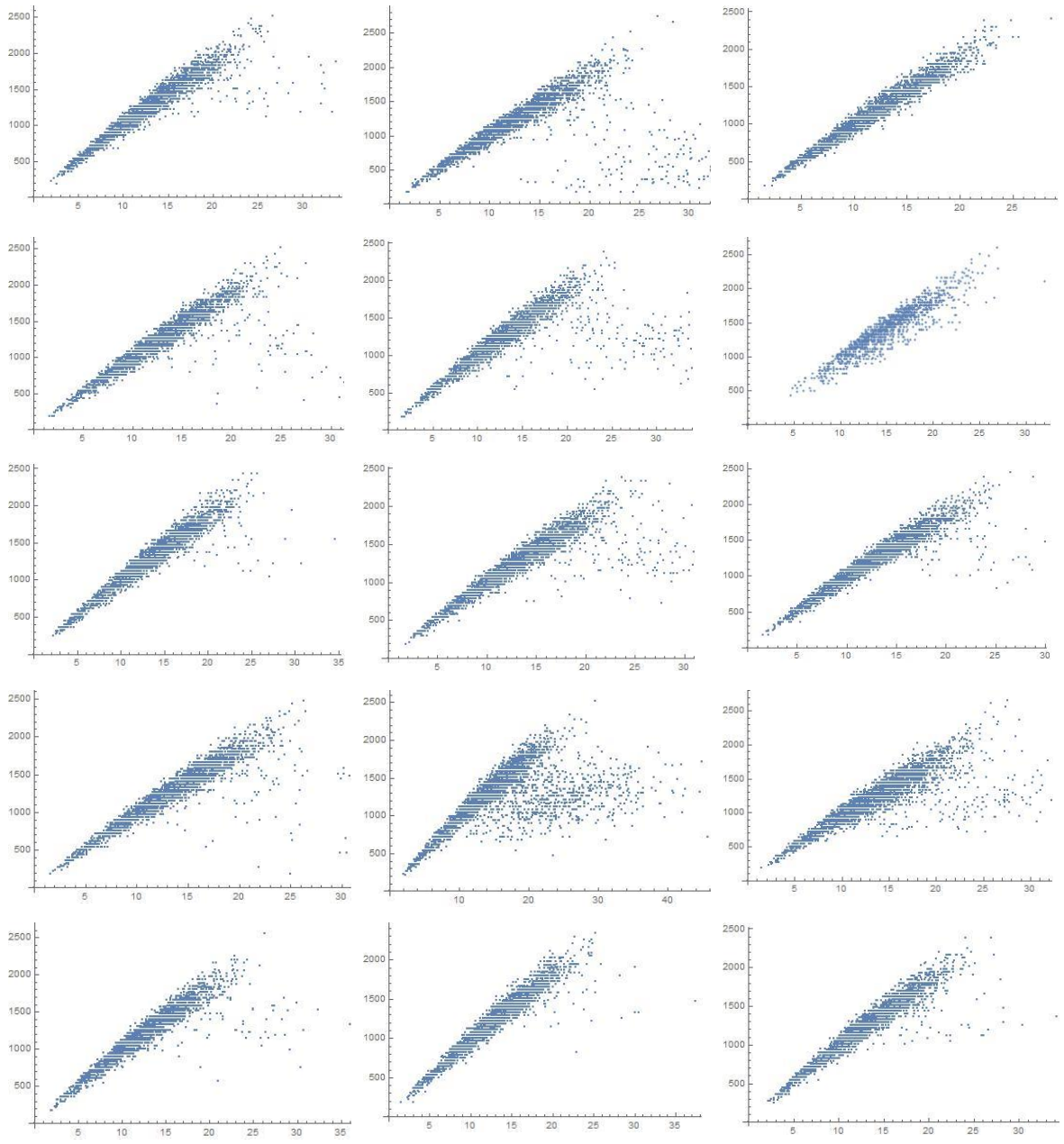

Figure 35 Flow-Occupancy (per lane) curve at D/S of Glenwood Road, April 2016. Flow is in vehicle/hr and occupancy is defined as the percentage of time that the sensor is occupied by a vehicle.